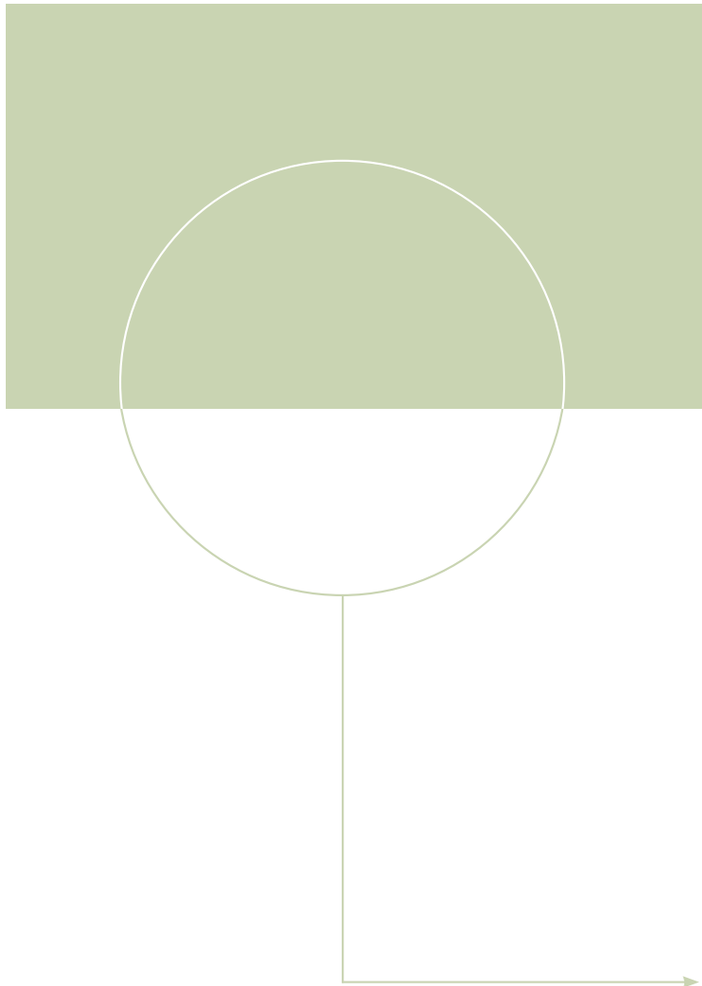

Master's thesis

2019

Shanjeevan Mohanarajah

NTNU
Norwegian University of
Science and Technology
Faculty of Engineering
Department of Geoscience and Petroleum

Shanjeevan Mohanarajah

AVO classification of facies and fluids constrained by burial history - Demonstrations on real data from Norwegian Shelf

June 2019

NTNU
Norwegian University of
Science and Technology

NTNU
Norwegian University of
Science and Technology

NTNU

Norwegian University of
Science and Technology

AVO classification of facies and fluids constrained by burial history - Demonstrations on real data from Norwegian Shelf

Shanjeevan Mohanarajah

MSc in Petroleum Geoscience and Engineering
Submission date: June 2019
Supervisor: Per Avseth

Norwegian University of Science and Technology
Department of Geoscience and Petroleum

NTNU

Norwegian University of
Science and Technology

AVO CLASSIFICATION OF FACIES AND FLUIDS CONSTRAINED BY BURIAL HISTORY - DEMONSTRATIONS ON REAL DATA FROM NORWEGIAN SHELF.

Master's thesis by candidate number: 10004

June 11, 2019

Abstract

This study is aimed to generate AVO classification of facies/fluids from Yttergryta to Natalia, and taking into account the burial history. To accomplish the objective, 3-stages workflow is followed. The study starts with Hampson Russell AVO, where we got the intercept and gradient for Yttergryta and Natalia. The next step is to do PeLe-modeling for porosity-depth trends for Yttergryta and Natalia, such that we get the elastic parameters for both of them. The last step is DigAVO, where we take in the outputs from Hampson Russell AVO and PeLe-modeling. Such that we could see the difference between Natalia and Yttergryta. Thereby, showcase how cementation affected both of them and to get the finale result visualizations of Yttergryta and Natalia.

Acknowledgments

We like to take this opportunity to express our gratitude to Norwegian University of Science and Technology - Trondheim for giving us the platform and resources to work on our master's thesis. Our sincere thanks to our supervisor, Professor Per Avseth, for his expertise and guidance during the course of this master's thesis.

A special thanks to our external partners, Dig Science and Lehocki Geospace, represented by Per Avseth and Ivan Lehocki for allowing us to use software like DigAVO and PeLe. In addition, a great gratitude to Tullow Oil for letting us use their released well data from the year 2015 for Yttergryta in this master's thesis.

Contents

List of Figures

List of Tables

1 Introduction

1.1 Objective of study

The main objective of the study is **to generate AVO classification of facies/fluids from Yttergryta to Natalia, and taking into account the burial history**. Burial history may vary spatially, and this should be taken into account during AVO classification.

1.2 Scope of study

1.2.1 Explore these issues

In this study we will explore about the subject of distinguishing gas, oil and water when the rock becomes stiff. The problem is that because of increased rigidity with depth, fluid sensitivity will decrease. Such that it becomes increasingly difficult to distinguish the different fluid classes with depth. Another factor is the variation when the rock gets increasingly stiffer under the burial sequence. The AVO-response will be different from two separate burial depths, and thereby the fluid classification would be different. The right respond is to correct AVO-response according to the right burial depth. This will be demonstrated on real seismic data from Yttergryta field located on the Norwegian shelf.

1.2.2 Research done before

There has been done a lot of research in this subject, such as: Per Avseth, Harald Fleische and Aart-Jan Van Wijngaarden in 2003 have done an article about AVO classification of lithology and pore fluids constrained by rock physics depth trends [Per Avseth and Wijngaarden, 2003]. In addition, Per Avseth and Ivan Lehocki in 2016 have an article about combining burial history and rock-physics modeling to constrain AVO analysis during exploration [Avseth and Lehocki, 2016]. General AVO-background is done in 2014 by Satinder Chopra and John P. Castagna [Chopra and Castagna, 2014]. There is a study done about the geology background of the Yttergryta field, which is Per Avseth, Andre Janke and Frederick Horn's article in 2016 about AVO inversion in exploration - key learnings from a Norwegian Sea prospect [Per Avseth and Horn, 2016]. In addition, are there master's studies done in this subject. Two different examples are Lara Antonia Blazevic Vucelic master's thesis on modeling burial induced changes in physical sandstone properties, and Taufik Maulana master's thesis on quantitative seismic interpretation using rock physics templates - case examples from the Zumba field.

1.2.3 Approach

The study begins with wells and the AVO-gathers loaded into the Hampson-Russell AVO. In addition, there was AVO-screening done here. Attributes are made here, such as intercept, gradient, product-stack with the intercept multiplied with the gradient, fluid factor, lithofactor, polygon classification. The last phase in Hampson-Russell was to make synthetic gathers to the well ties. Thereby, showcase the AVO-gathers are right to the well ties, Natalia and Yttergryta.

The next step was PeLe, where Yttergryta and Natalia well log data gets uploaded. In this phase, burial-constrained AVO-analyze was conducted. Values of V_p, V_s and ρ for the different fluid classes are found here.

The last step was DigAVO, where the input was R(0) + G from Hampson-Russell. In addition, we used the PeLe-results to get the training data by Monte Carlo-simulation, and finalized it with AVO-classification of facies/fluids. Then we could test it to see the difference between Natalia and Yttergryta.

1.2.4 Beneficial for the future

This study could benefit others by that we look at Yttergryta field with new eyes, and thereby understand more about near field. There can be more potential in the area, and our method can benefit others in the future by having more access to information about Yttergryta field.

1.3 General field overview

Yttergryta field is located in eastern part of Halten Terrace, roughly 270 kilometres off the Norwegian coastline. The field was discovered by Statoil ASA (old, Equinor now) in 2007 by well 6507/11-8. The production phase of Yttergryta field started in January of 2009 and ended in June 2012. Equinor (operator), Total, Petoro and Vår Energi are the companies that has the right of the licences of Yttergryta field. [NPD, 2019]

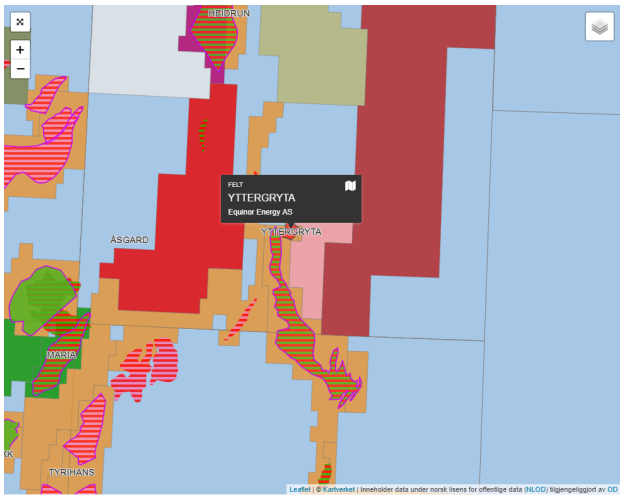

(a) Field area of Yttergryta

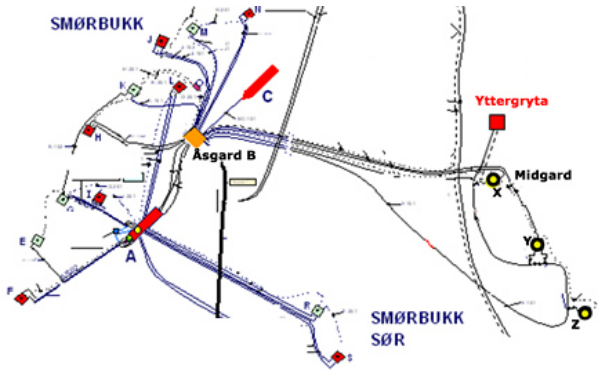

(b) Development and operation (PDO) of Yttergryta field

Figure 1: This shows the area and PDO of Yttergryta field [NPD, 2019]

Figure 1*b* shows the PDO of Yttergryta field in the Norwegian Sea, 33 kilometres east of the Åsgard B platform, was approved in 2008. It was developed with a subsea template, which was connected to the Åsgard B platform. In addition, it was connected through the Midgard X-template. The water depth is around 300 metres. [NPD, 2019]

Yttergryta field consists of three reservoirs - Garn, Not and Ile Formations. The lithology down to the top of Garn Formation at 2416 meters was with no reservoir quality, because it had primarily

claystone there. The petrophysical evaluation of those three formations gave the results that showed high hydrocarbon saturation with good reservoir quality with 28 percent porosity and permeability up as 6 Darcy there. The reservoir was in dynamic stage of depletion, which was shown by the Molar Formation Dynamic Tester (MDT) pressure data. This situation occurred due to production from Åsgard field, which come from the Midgard discovery. The MDT gas/condensate sample were taken at 2424 meters showed that condensate/gas ratio= 2070 Sm3/Sm3, condensate density=0.792 g/cm^3 and gas gravity= 0.695. [NPD, 2019]

In Yttergryta field, a gas down-to situation was confirmed. In the target reservoir were there gas, but no significant oil were indicated in the well. Yttergryta field produced gas from sandstone Middle Jurassic age in the Fangst group. 2400 - 2500 metres was the depth of the reservoir. The field was produced by pressure depletion. From the template Midgard X, the gas was transported to the Åsgard B to be processed. Because the gas from the Yttergryta had a low CO2 content, made it suited for dilution of CO2 in the Åsgard Transport System (ÅTS). [NPD, 2019]

In 2010 at Yttergryta field, the production stopped because of water breakthrough in the gas production well. A restart of the production happened in 2012 and failed, this lead to that Yttergryta field was permanently shut down. It will be disconnected from the Midgard template and will be decommissioned at the same time as the Åsgard facilities.[NPD, 2019]

The well 6507/11-9 called Natalia was drilled by StatoilHydro AS in April in 2008 to prove the presence of hydrocarbons in Jurassic sandstone in the Fangst Group. In addition, to examine the migration route for the hydrocarbons in the prospect area. In April 2008, the well was abandoned as a gas discovery. [Oljedirektoratet, 2019]

2 Geological setting

Yttergryta field is located at the border between Halten Terrace and Trønderlag Platform in the Norwegian Sea. It lies within PL 591 and PL 263 license. In addition, it covers Høgbraken horst and Grinda graben by many normal faults.

Figure 2 shows the stratigraphic of this study is from Lower Jurassic to the Base Cretaceous Unconformity. In addition, Figure 2 shows the three groups for our study. They are Båt Group, Fangst Group and Viking Group.

In Båt Group we have in our study formations like Tilje Fm and Ror Fm. The Ror Fm consists for the most of grey to dark mudstones with some sandy and silty sequences. It is primarily a seal for Tilje Fm and the thickness of the formation is around 70 to 170 meters. The deposition of Ror Fm happened in open shelf environments below wave base in Lower Jurassic age. The Tilje Fm consists of sandstones interbedded with shale and siltstones. The thickness of it's 100 to 150 meters, and it was deposited in nearshore marine to intertidal environments. [Center, 2019]

The Ile Fm, Not Fm and Garn Fm are in the Fangst group. Here we will find three main reservoirs that we would focus on in this study. The Garn Fm consists of medium to coarse grained sandstones with interlayered mica-rich zones. That haven been deposited in a near shore wave with shallow marine environment in the Middle Jurassic age, and the thickness of Garn Fm is around 104 to 150 meters. The Not Fm is kind of seal for the Ile Fm, because it consists of transgressional marine claystone. The Ile Fm consists of medium to coarse sandstone and it was deposited on the Middle Jurassic age. [Center, 2019]

In Viking Group we find the Melke Fm and Spekk Fm. They are seals for the Garn Fm. The Melke Fm consists of dark mudstones interbedded with some limestones and siltstones. In Upper Jurassic age, the Melke Fm have been deposited in an open marine environment. The Spekk Fm one will find in Upper Jurassic to Lower Cretaceous age, and it consists of organic shale that have been deposited in marine anoxic bottom water.[Center, 2019]

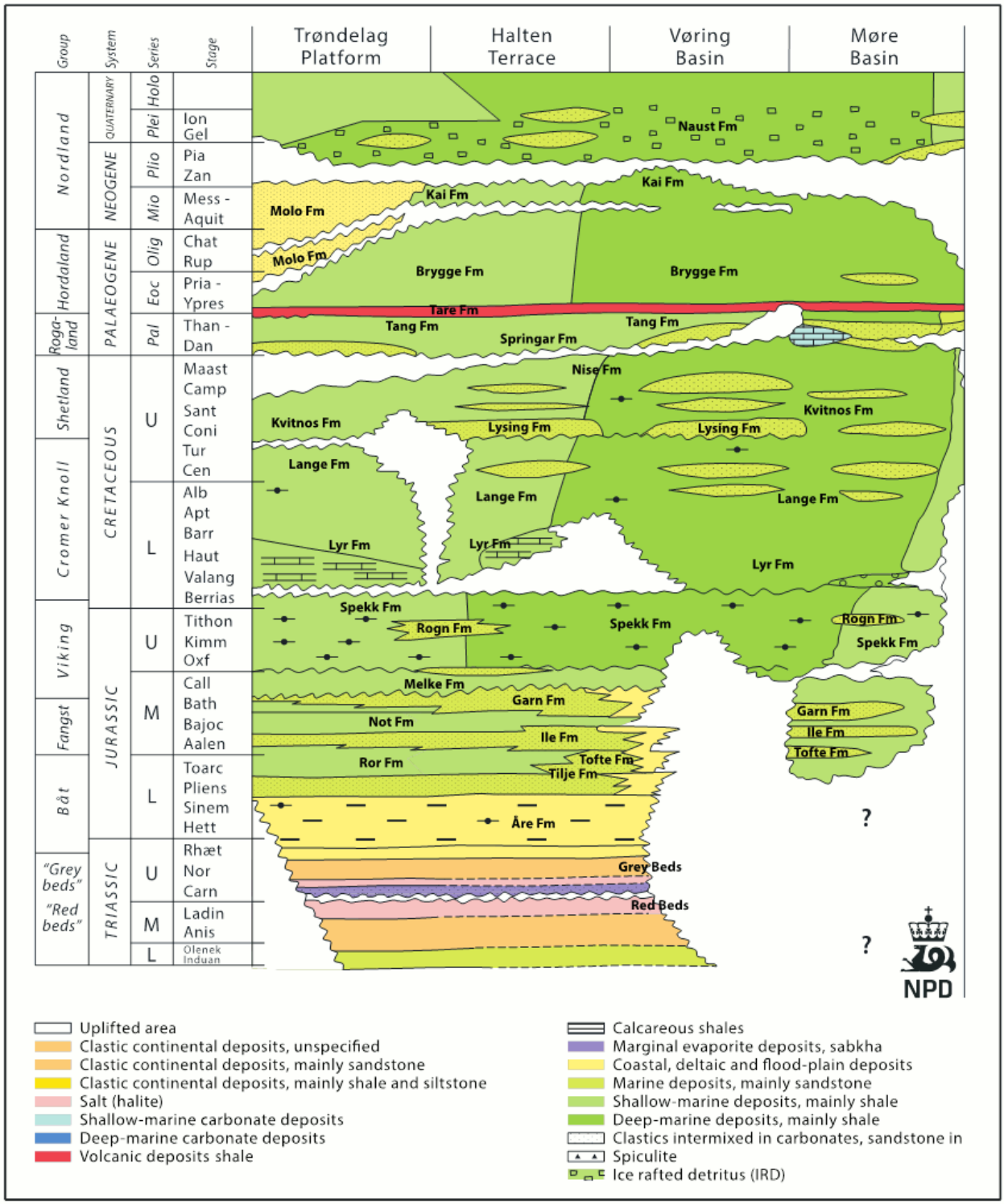

Figure 2: Lithostratigraphic overview of the Norwegian Sea Shelf area [Center, 2019]

3 Theory

3.1 Compaction processes

In a compaction process, there are two processes that occur. That is mechanical compaction and chemical compaction, and that is shown on Figure 3

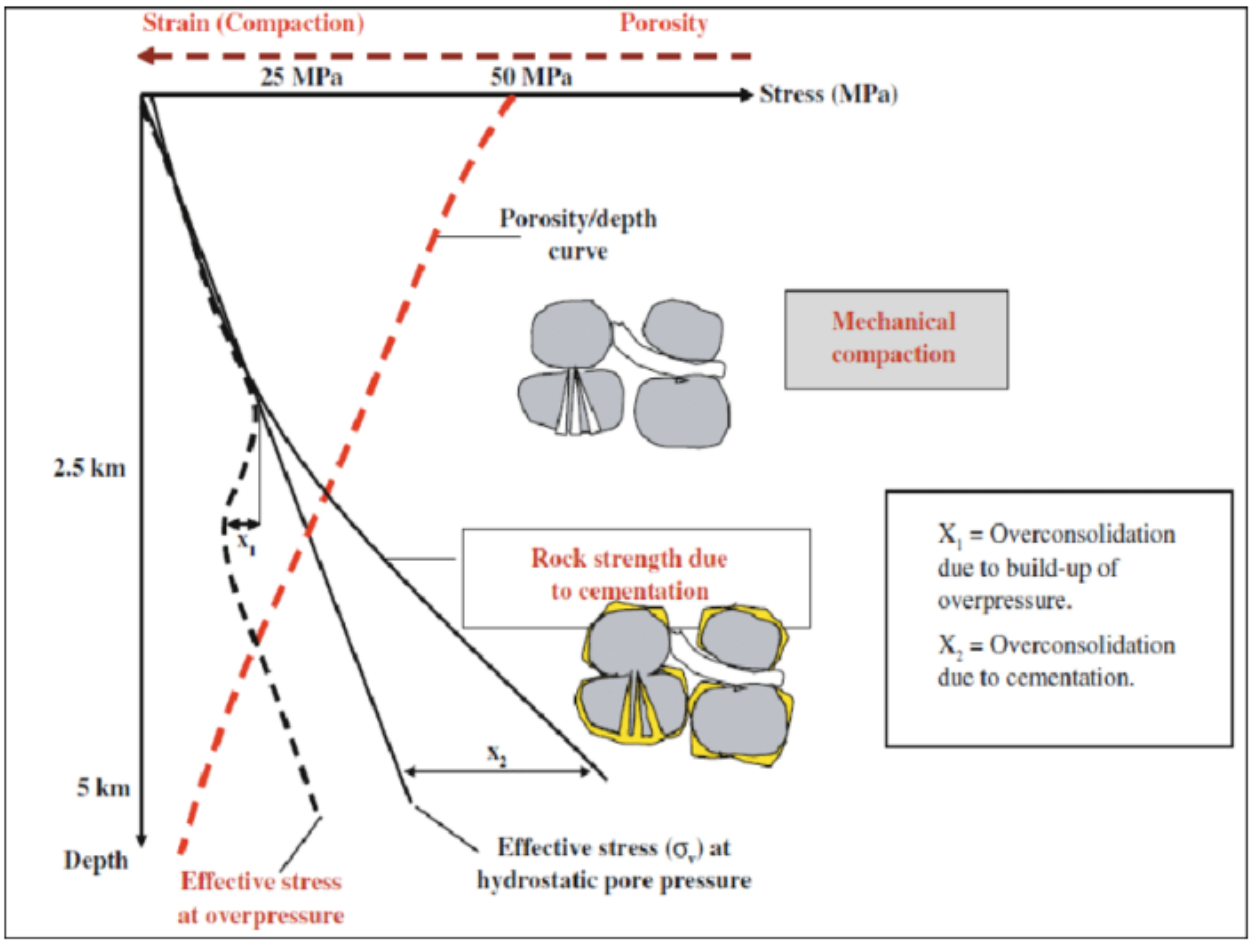

Figure 3: Mechanical compaction at shallow depth and chemical compaction at 70 degree Celsius [Bjørnlykke and Jahren, 2010]

Figure 3 shows mechanical compaction as a function of effective stress by grain breakage and grain reorientation at shallow depth. After 2-2.5 kilometers one will get chemical compaction at temperature around 70 degrees Celsius and cementation occurs. For sandstone the compaction is the reduction in the bulk rock volume by these processes [Walderhaug and Lander, 1999]: grain rearrangement, plastic deformation, dissolution and brittle deformation. Grain rearrangement makes the grain framework move to a tighter packing configurations with the correlation of the stress transmitted through the framework grains. When the grains deform is it because of the stress, then plastic deformation occurs under the bulk compaction. During this situation the consolidation occurs because the pores collapse or are invaded by deforming grains, and this gives further grain rearrangement [Walderhaug and Lander, 1999]. Brittle deformation plays just a minor role in

compaction [Walderhaug and Lander, 1999].

In chemical compaction, the cementation starts and then the process of dissolution of the grains occurs. The quartz surface area reduces by increasing grain contact area in the compaction, and the injection of matrix material into pore spaces. Cementation can cause surface area reduction when quartz grains are encased by pore-filling cements [Walderhaug and Lander, 1999]. The equation of the quartz cementation is given by this equation [Walderhaug, 1996]:

$$V_{cem} = \phi_{0cc}[1 - exp[\frac{MaA_0}{\mu\phi_{0cc}bln10}(10^{bt_2} - 10^{bt_1})]] \quad (1)$$

Where V_{cem} is the volume(cm^3) of quartz cement, and ϕ_{0cc} is the porosity at the start of cementation. M is the molar mass of quartz (60.09 $\frac{g}{mole}$), and a and b are constants with units of $\frac{moles}{cm^2}$ and $\frac{1}{C^0}$ for both of them. C is the heating rate ($\frac{C^0}{Myr}$), and at last the temperatures for an given interval are T_1 and T_2.

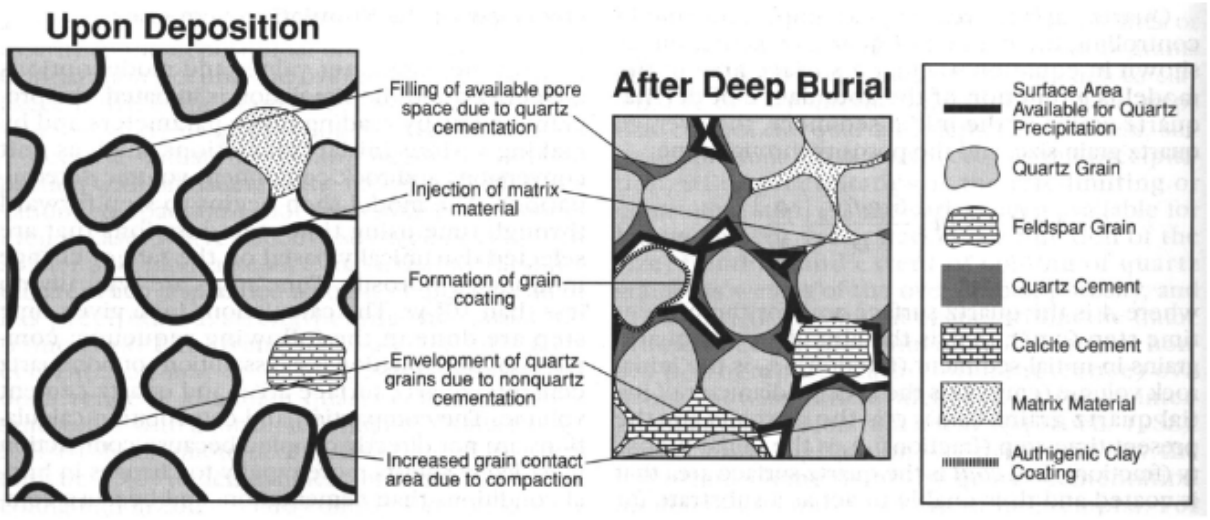

Figure 4: Causes of surface area reduction during sandstone diagenesis [Walderhaug and Lander, 1999]

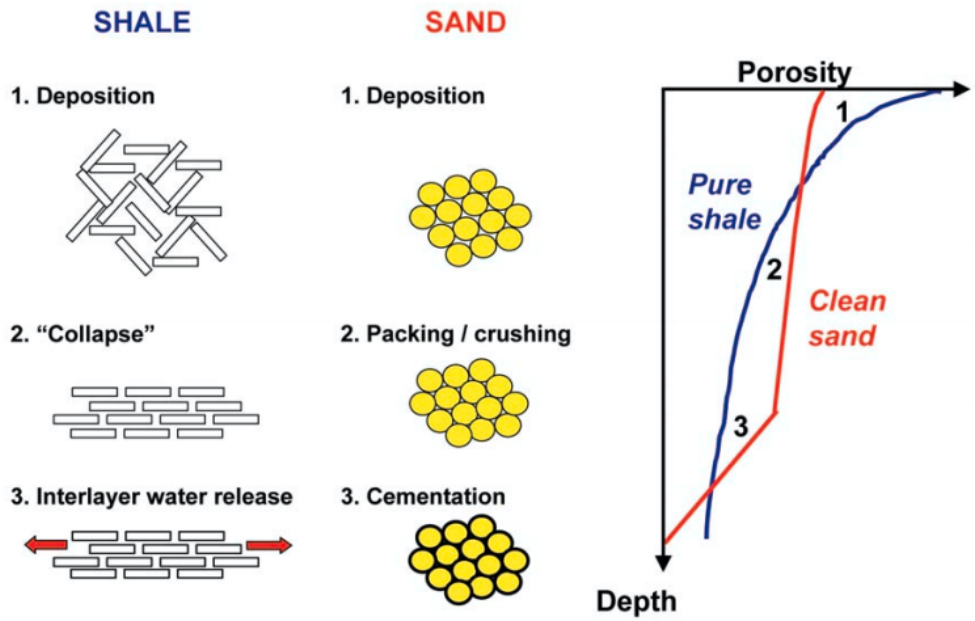

Figure 5: Scheme of porosity-depth trends for sand and shale [Per Avseth and Wijngaarden, 2003]

The porosity-depth trends for sand and shale are shown in Figure 5. The trends for sand and shale can change much because of the composition, temperature, texture, pore fluids and pressure gradients. At the points between 1 and 2 on the curve of Figure 5 is mechanical compaction. It shows how sand and shale behaves in the mechanical compaction zone as the depth increases. The point 3 illustrates the chemical compaction when the cementation occurs, and a natural consequence of that is that the porosity decays a lot for sand. Usually for sandstone this occurs at 70 degrees Celsius. The porosity as a function of burial depth can be expressed like this [Per Avseth and Horn, 2016]:

$$\phi(Z) = \phi_0 exp(-cZ) \tag{2}$$

where ϕ is the porosity at burial depth, ϕ_0 is the critical porosity, Z stands for depth, and c is the exponential decay constant.

3.2 Gassmann fluid substitution

The formula for the Gassmann fluid substitution is given in this equation [Gassmann, 1951]:

$$\frac{K_{sat}}{K_m - K_{sat}} = \frac{K_{dry}}{K_m - K_{dry}} + \frac{K_f}{\phi(K_m - K_f)} \tag{3}$$

Where the K_{dry}= dry rock bulk modulus, K_m=mineral bulk modulus, K_f=pore fluid bulk modulus and ϕ is the porosity. The Gassmann equation is a necessary tool to predict the velocity changes culminated from different fluid saturations.

3.3 Seismic velocities

Seismic velocity is the speed which an elastic wave propagates through a medium. The seismic velocity increases with increasing depth, and it varies though rock type and fluid. These are formula for the seismic velocities for P-wave velocity, S-wave velocity and bulk density are given here [Landrø, 2011]:

$$V_p = \sqrt{K + \frac{(4/3)\mu}{\rho}} \tag{4}$$

$$V_s = \sqrt{\frac{\mu}{\rho}} \tag{5}$$

$$\rho = \phi\rho_{fluid} + (1-\phi)\rho_{mineral} \tag{6}$$

Where K is the bulk modulus, μ is the shear modulus and ϕ is the total porosity.

3.4 AVO

Amplitude variation offset (AVO) analysis is a concept used in exploration and reservoir seismic. AVO is mainly the variation in seismic amplitude with change in distance between airgun shots and receivers. It is conducted on CMP gather or partial stacks. Figure 6 shows how a seismic wave is reflected at an interface, and the reflectivity varies as a function of the incidence angle. In addition, the Figure 6 shows P-wave and S-wave reflected at the interface, and when it's transmitted [Landrø, 2011].

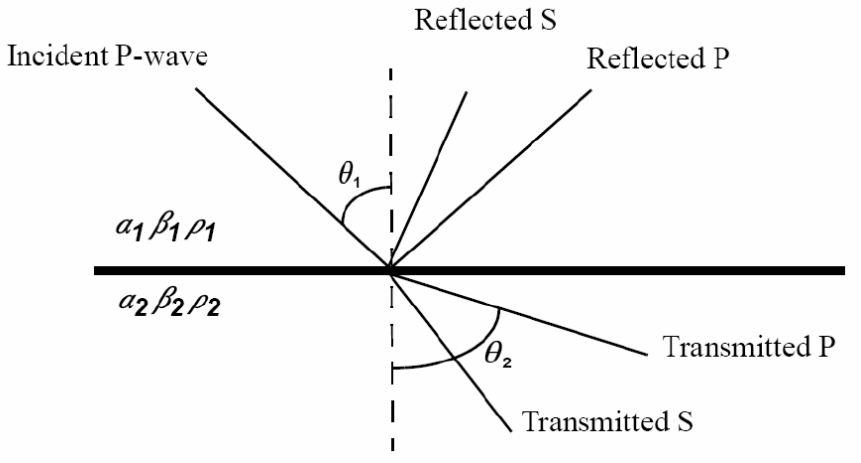

Figure 6: Overview of reflection and transmission for P-wave and S-wave at an interface [Landrø, 2011]

Where we have the α and β denote as P-and S wave velocity, ρ = density and θ = incidence angle for each layer.

From the Zoeppritz equations (Zoeppritz 1919) we can get the reflection and transmission coefficients. They are very complicated, which have been approximated and linearised by Shuey [Sheuy, 1985] and others into this term that describes the angle dependent reflectivity:

$$R(\theta) = R(0) + Gsin^2(\theta) \tag{7}$$

R(0) is the zero offset reflectivity at a given seismic horizon, controlled by the contrast in acoustic impedance (AI) across this interface:

$$R(0) = \frac{AI_2 - AI_1}{AI_1 + AI_2} \tag{8}$$

AI_1 and AI_2 stands for the acoustic impedances for layer 1 and layer 2. AVO gradient stands for G here, which is affected by the contrast in V_p/V_s ratios across the same interface:

$$G = \frac{1}{2}\frac{\Delta V_p}{V_p} - 2\frac{V_s^2}{V_p^2}(\frac{\Delta\rho}{\rho} + 2\frac{\Delta V_s}{V_p}) \tag{9}$$

From AVO we can get information about the burial depth, lithofacies and pore fluid, which is essential in this study.

3.5 AVO classes

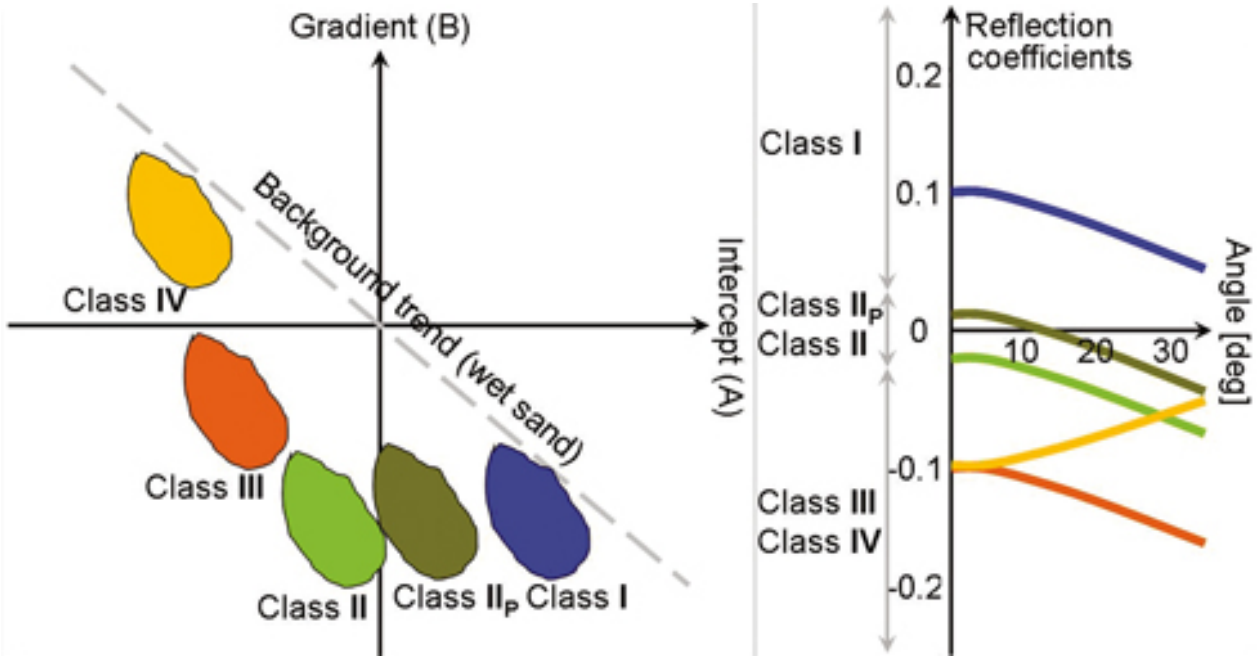

Figure 7: Scheme of the AVO classes in a cross plot [Per Avseth and Mavko, 2005]

Figure 7 shows AVO classes in a cross plot. Where class I is for high-impedance reservoirs, class II is for near-zero impedance reservoirs and class III & class IV is for low-impedance reservoirs [Rutherford and Williams, 1989].

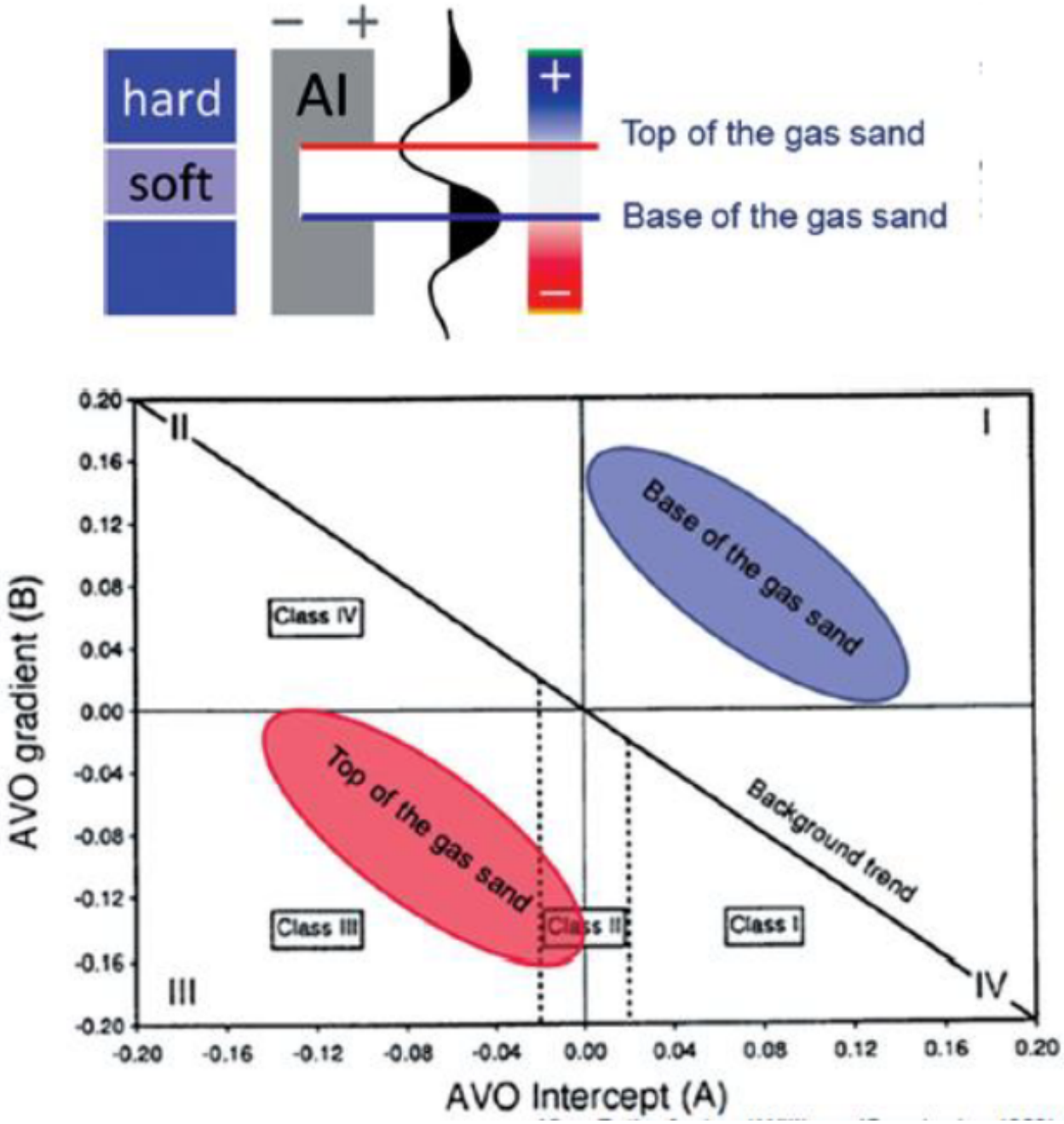

Figure 8: Scheme of the AVO classes in a cross plot [Rutherford and Williams, 1989]

Figure 8 shows AVO classes in the cross plot with the top and the base of gas sand. In addition, the polarity for these in seismic responses. Where in the third quadrant in class III we have gas at bottom, then oil and brine close to the background line. The background line is a indicator for the fluid line. But in the first quadrant, it's flipped because of opposite sign. Gas at the top, then oil and brine close to the fluid line [Rutherford and Williams, 1989].

4 Methodology

In this study we used 3-stages workflow. The workflow of this study is shown in Figure 9.

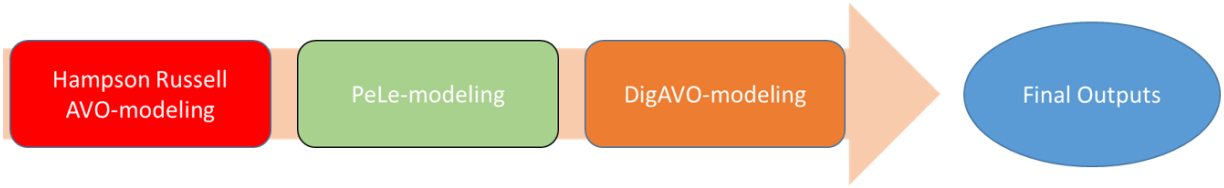

Figure 9: Workflow of the study

This study started with Hampson Russell AVO-modeling, where we loaded in the real seismic data that we got from Tullow Oil. The seismic data consists of xline 2508 Yttergryta, inline 2096 Yttergryta, xline 2947 Natalia and inline 2278 Natalia. We started first with one data sett at time. Then we applied first the well information into the software for each of them, and that is shown in Table 1.

Table 1: Well information for Yttergryta and Natalia [NPD, 2019]

Parameter	Yttergryta	Natalia
NS UTM [m]	7221898.70	7226521.88
EW UTM [m]	429994.97	425900.64
Kelly bushing [m]	24	18
Water depth [m]	300	281

In Hampson Russell AVO under seismic processing under utilities, we find the section for trace maths. Here we put the ranges for angle stack near was 5-15 degrees and for angle stack far was 25-35 degrees for the seismic data. Then we had to correct the amplitude by multiplying it with -1, and called then cN and cF. Such that the hard reflector was red colour and softer reflector was blue colour. For the gradient, fluid factor and lithofactor we applied these: cG= cF*1.4 - cN, FF= cN + 1.3*(cF-cN) and LF= cN - 0.85*(cF-cN). Such that we made trace maths for every corrected line in near, far, gradient, fluid factor and lithofactor.

In addition, in Hampson Russell AVO under seismic processing under cross plotting, we find the section for cross plot seismic. Here we did the polygon classification for each line. In the polygon classification we picked out the area for the different fluid classes according to the AVO class figures like Figure 7 and Figure 8. Then we extracted the intercepts and gradients for each line in CDP and TWT in Hampson Russell AVO for further use in DigAVO.

The next step was PeLe-modeling. Here we uploaded the well log data for Yttergryta and Natalia into the software. In the main setting we put the normal setting for the seismic parameters. Such that the seismic responses would appear in PeLe. In the zonate table we used the values for top and base for the different formations as shown in Table 2 and Table 3.

Table 2: Values to Yttergryta used in zonate section in PeLe-modeling [NPD, 2019]

Formation	Top [m]	Base [m]
Lyr	2359	2373
Spekk	2373	2391
Melke	2391	2416
Garn	2416	2447
Not	2447	2459
Ille	2459	2519
Ror	2519	2594
Tilje	2594	2701

Table 3: Values to Natalia used in zonate section in PeLe-modeling [Oljedirektoratet, 2019]

Formation	Top [m]	Base [m]
Lyr	2531	2535
Spekk	2535	2543
Melke	2543	2597
Garn	2597	2637
Not	2637	2653
Ille	2653	2730
Ror	2730	2812
Tilje	2812	2910

In this study the interesting formations used in PeLe was from Melke Fm and down to Tilje Fm. The formation sections on the graphs was colored with different colors. The most obvious one were Garn Fm with yellow gas sand and Tilje Fm with blue brine sand. The aim then to get the seismic responses on right formation depth. This was done in Yttergryta by setting burial depth at 2090 meters, kelly bushing at 24 meters and water depth at 300 meters [NPD, 2019]. In Yttergryta we followed these depth, such that we could get the right seismic response at right depth with the V_p/V_s around 1.8-1.9 to the shale at Melke Fm. In addition, the illite values was boosted to get that as well. In Natalia we put the burial depth at 2301 meters, kelly bushing at 18 meters and water depth at 281 meters [NPD, 2019]. We picked values from a softer shale in Natalia In this case we tested with a softer Spekk type shale, to see if it was possible to catch Rogn sand in graben structures. In addition, to see the possibility of softer Cretaceous shale that can sometimes lie right on Jurassic sand. From PeLe-modeling we got the seismic outputs like V_p, V_s, porosity, AI, V_p/V_s ratio, V_p/V_s ratio versus AI and gradient versus intercept according to the burial history at depth by results visualization. Then we picked values for V_p, V_s and density (ρ) for Yttergryta and Natalia to used further in DigAVO.

The last step was DigAVO, where we took in the intercept and gradient from Hampson Russell AVO-results. In addition, the Pele-results to get the training data by Monte Carlo-simulation. Then we did the calibration for the real data and the training data. Such that we got the AVO-classification of facies/fluids by results visualization for Yttergryta and Natalia.

5 Results

5.1 Hampson Russell AVO

In this section we start with the step by step results for inline 2096 Yttergryta, and compliments with the final results for xline 2508 Yttergryta, inline 2278 Natalia and xline 2947 Natalia. By doing AVO-screening we can showcase the AVO-gathers are right to the well ties for Yttergryta and Natalia. The end product is to get the intercept and gradient from Hampson Russell AVO and load it into DigAVO for final AVO-classification of facies/fluids.

5.1.1 Hampson Russell AVO results for inline 2096 Yttergryta

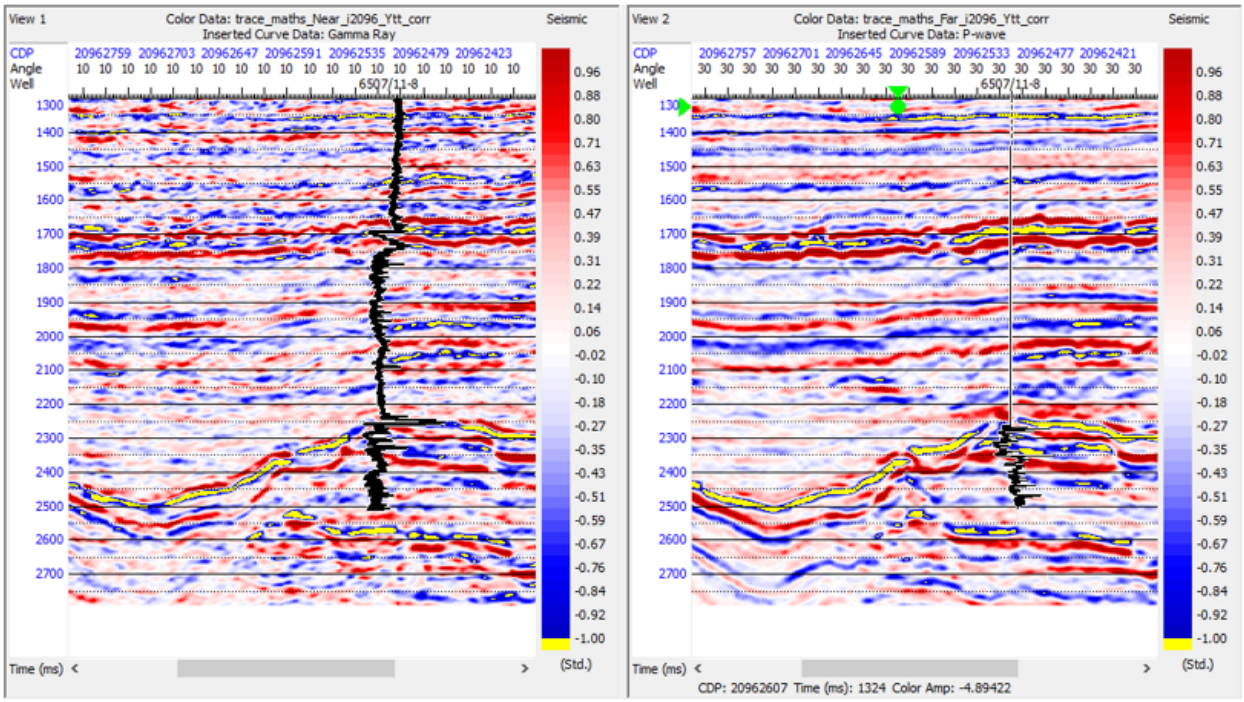

Figure 10: The comparison between corrected near stack gathers and corrected far stack gathers at inline 2096 Yttergryta

Figure 10 shows the comparison between corrected near stack gathers and corrected far stack gathers at inline 2096 Yttergryta. The amplitude are corrected and that is normalizing. We can see controlled effect on the corrected far stack. The red colour is hard reflector, blue colour is softer reflector and yellow colour is the softest reflector. We see the graben structure clearly, and the yellow reflector shows the reservoirs. Especially for the Garn Fm around 2420 meters. The black line is the well log to Yttergryta. There we can see on the corrected near stack gathers, that the curvature of gamma ray spikes up around when it hits Melke Fm at around 2370 meters.

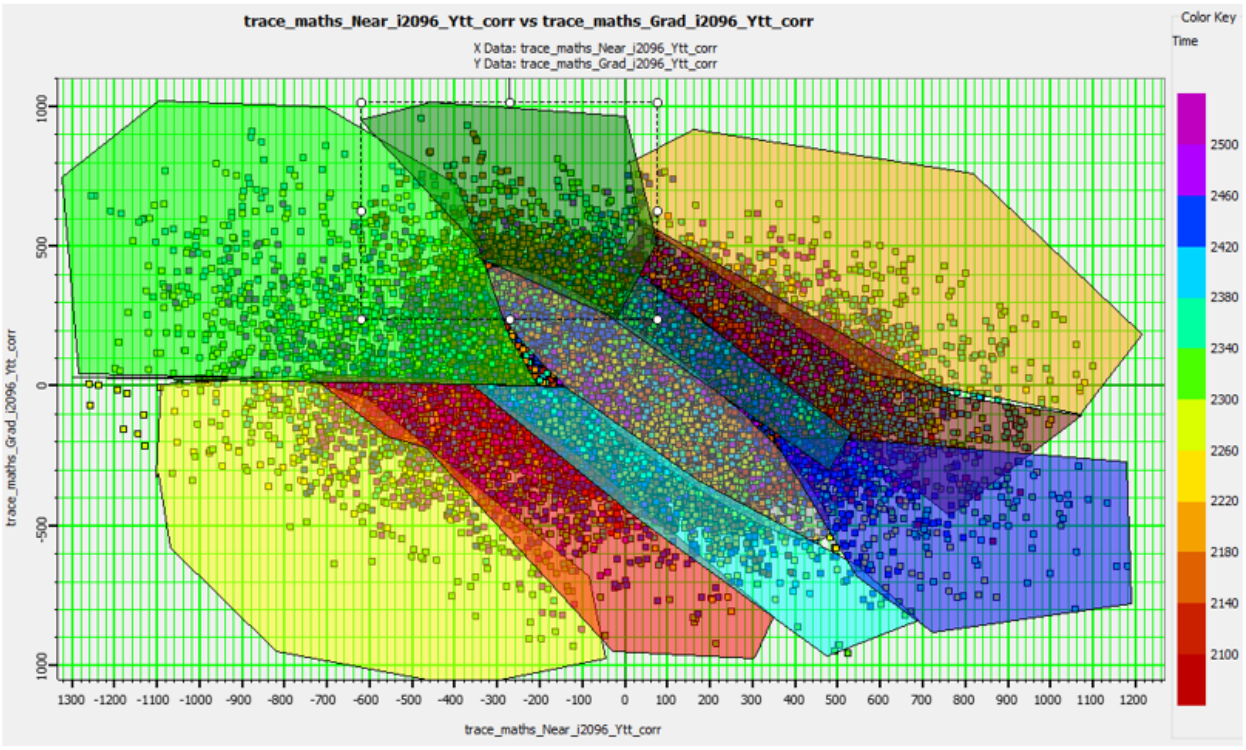

Figure 11: Polygon classification for the cross plot for the intercept and gradient at inline 2096 Yttergryta

Figure 11 shows cross plot for the intercept and gradient at inline 2096 Yttergryta, and polygon classification has been conducted by defining areas for different AVO classes for different fluids. The eclipse in the middle on Figure 11 shows the background trend for the most of data that lies there. Class III on Figure 11 are the colour yellow for gas sand, colour red for oil sand and light blue is for brine sand. Green colour is shale at class IV and dark green colour is hotshale on Figure 11. The bottom response to hydrocarbons is orange, and dark blue is for carbonates on Figure 11. This same definitions is applied for the polygon classification on xline 2508 Yttergryta on Figure 14 at late stage in this study.

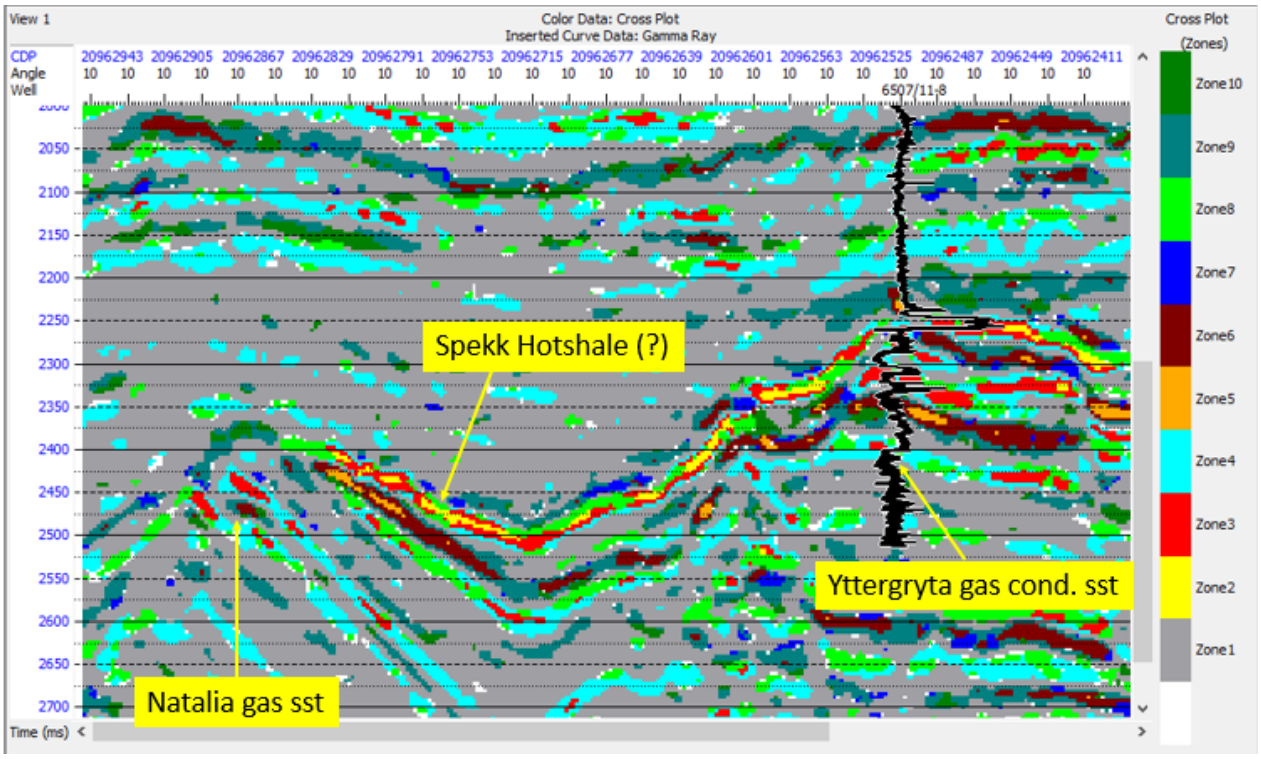

Figure 12: Result visualization from Hampson Russell AVO of inline 2096 Yttergryta

Figure 12 shows on the left side the Natalia gas sandstone with the red flat spots. The Yttergryta gas condensate sandstone are on the right side where the yellow arrow points to the spot. It's a red flat spot that lights up. We can see the graben structures clearly. But the Spekk hotshale is so thin in this study, because we lack logs through it.

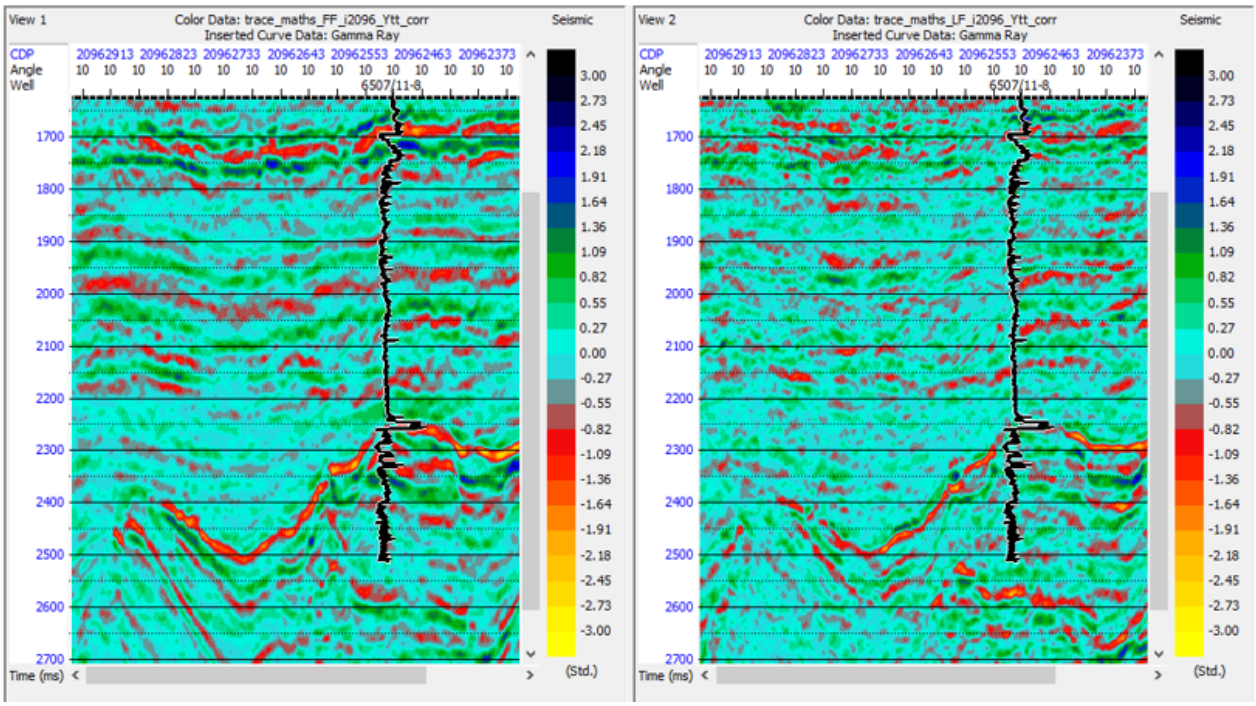

Figure 13: The comparison between fluid factor and lithofactor at inline 2096 Yttergryta

Figure 13 shows the comparison between fluid factor and lithofactor at inline 2096 Yttergryta. On the left side we see the fluid factor and there we see different fluids lights up at different stages. When compared to the right side we see the lithofactor, where the fluids are gone on the different stages from the left side to the right side. Then we only have the lithofactor left, and only the different lithologies is in sight.

5.1.2 Hampson Russell AVO results for xline 2508 Yttergryta

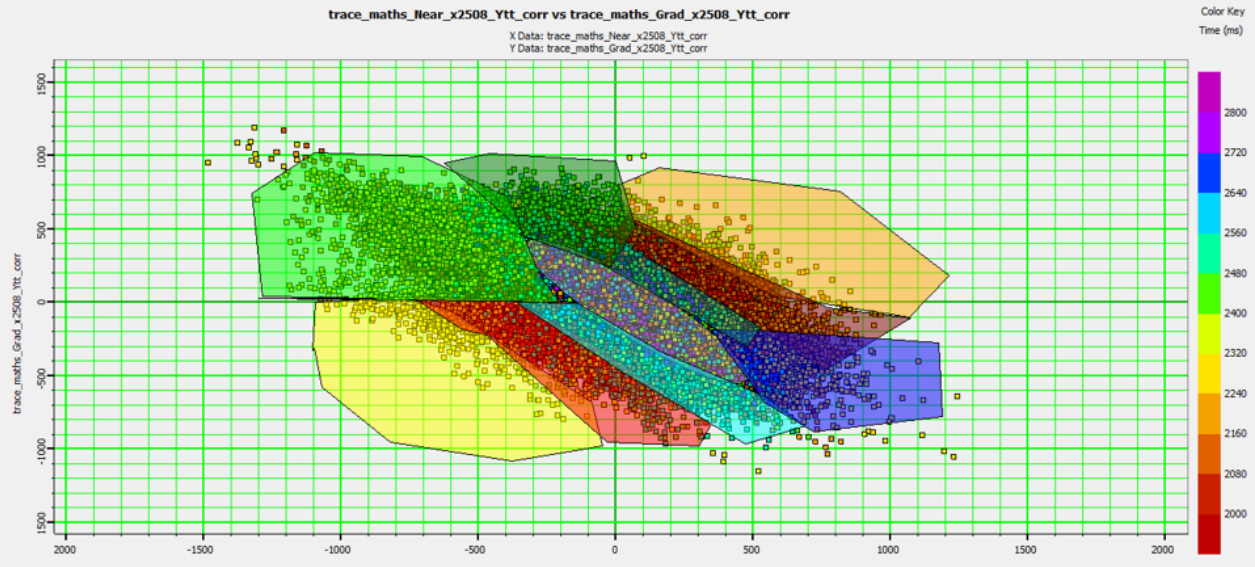

Figure 14: Polygon classification for the cross plot for the intercept and gradient at xline 2508 Yttergryta

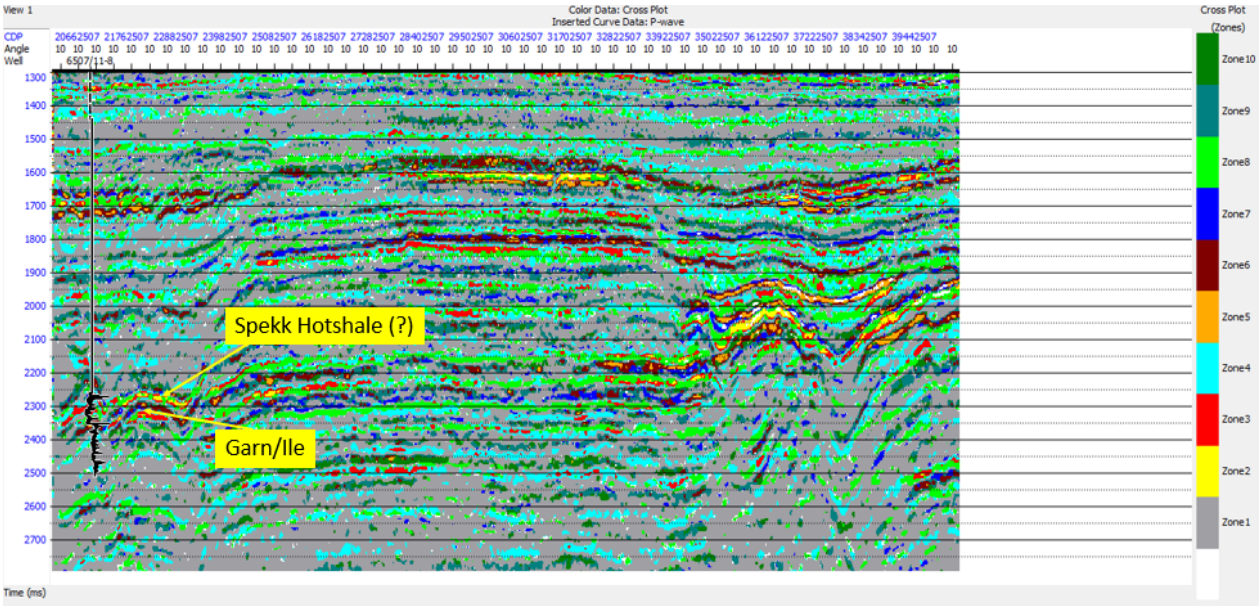

Figure 15: Result visualization from Hampson Russell AVO of xline 2508 Yttergryta

Figure 15 shows the result visualization from Hampson Russell AVO of xline 2508 Yttergryta. We can see clearly the fluid contact in Yttergryta. The gas and gas condensate sandstones in Garn Fm and Ile Fm shows really well on Figure 15. In addition, we can see the Spekk Hotshale there as well.

5.1.3 Hampson Russell AVO results for inline 2278 Natalia

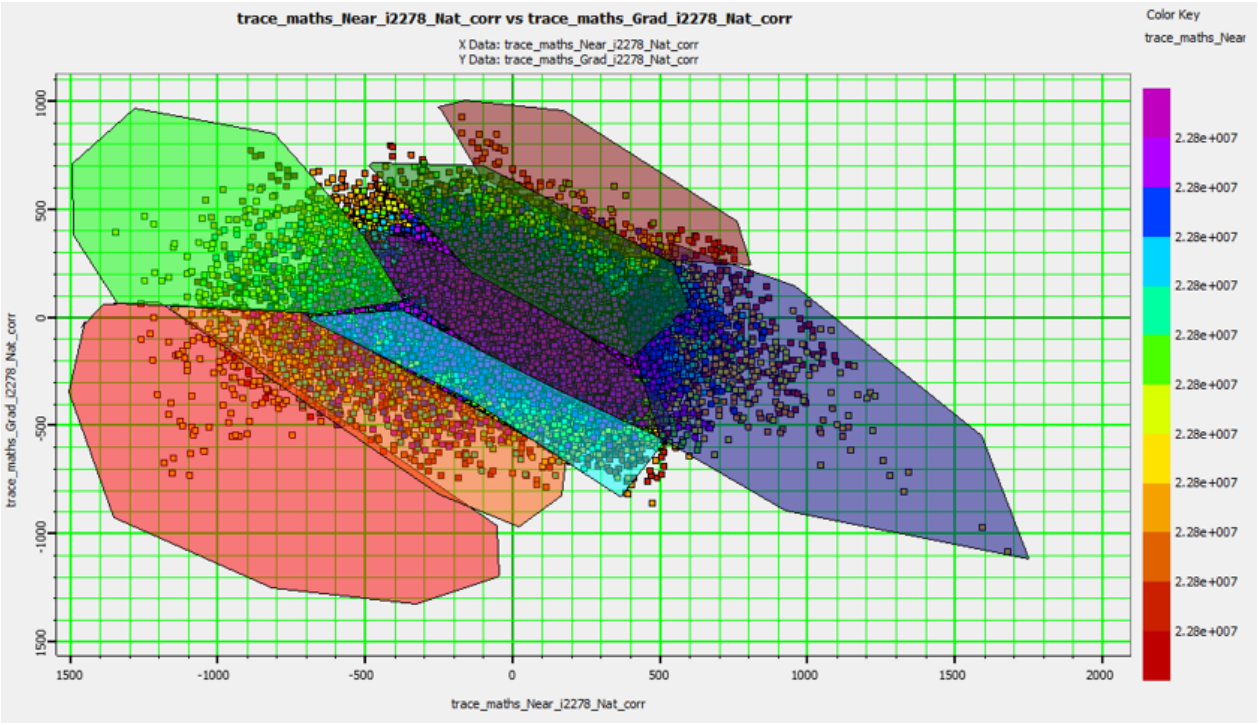

Figure 16: Polygon classification for the cross plot for the intercept and gradient at inline 2278 Natalia

Figure 16 shows cross plot for the intercept and gradient at inline 2278 Natalia, and polygon classification has been conducted by defining areas for different AVO classes for different fluids. The eclipse with the purple colour in the middle on Figure 16 shows the background trend for the most of data that lies there. Class III on Figure 16 are the colour red for gas sand, colour orange for oil sand and light blue is for brine sand. The green colour is shale at class IV. The bottom response to hydrocarbons is dark red, and dark blue is for carbonates on Figure 16. This same definitions is applied for the polygon classification on xline 2947 Natalia on Figure 18 at later stage in this study..

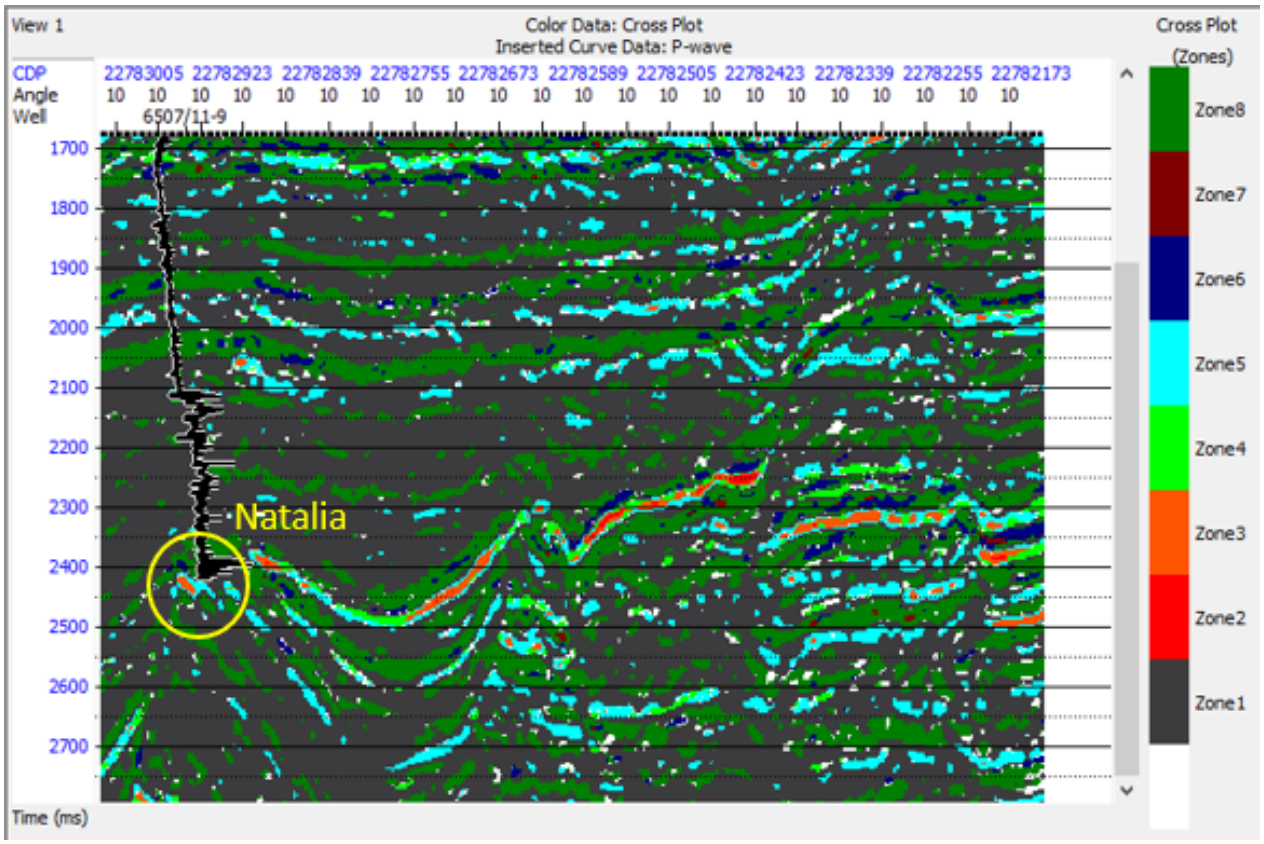

Figure 17: Result visualization from Hampson Russell AVO of inline 2278 Natalia

The result visualization from Hampson Russell AVO of inline 2278 Natalia is shown in Figure 17. The condensate gas sandstone one can see clearly by the red flat spot in Natalia on Figure 17. It's difficult to do interpretation of Natalia, because of the cementation. The cementation occurred just right above the reservoirs for Natalia. We see that downwards from the reservoirs, the more difficult it becomes to find the hydrocarbons due to the cementation. We only see clearly the red flat spot in yellow circled line on Figure 17.

5.1.4 Hampson Russell AVO results for xline 2947 Natalia

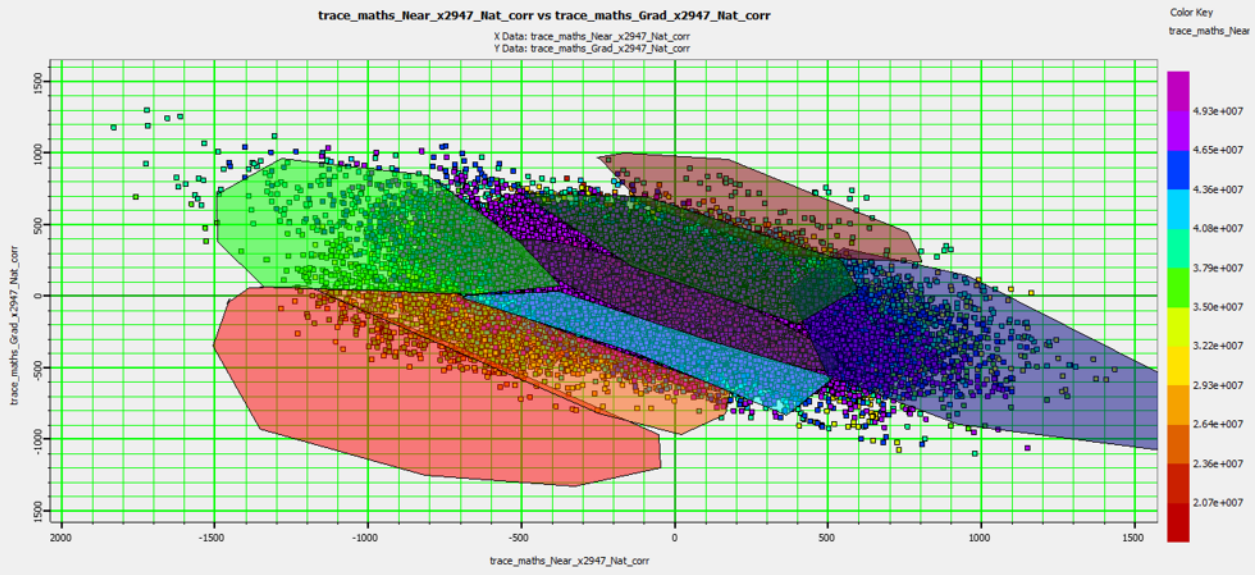

Figure 18: Polygon classification for the cross plot for the intercept and gradient at xline 2947 Natalia

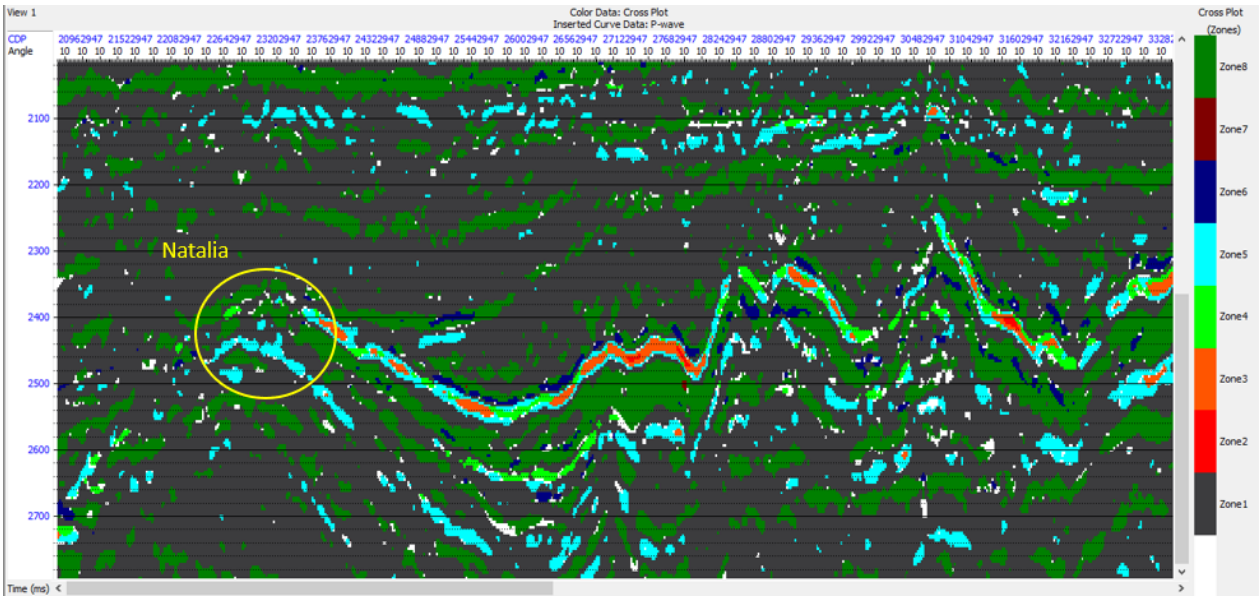

Figure 19: Result visualization from Hampson Russell AVO of xline 2947 Natalia

Figure 19 shows result visualization from Hampson Russell AVO of the xline 2947 Natalia. There we can see no hydrocarbons at the yellow circle at xline 2947 Natalia. Flat spots appear under the graben structures. But Figure 19 shows the structures are affected by cementation just above the reservoirs and downwards in Natalia. We can't see the hydrocarbons and the structures good enough.

5.2 PeLe-results

In PeLe-modeling one get the seismic outputs like V_p, V_s, porosity, AI, V_p/V_s ratio, V_p/V_s ratio versus AI and gradient versus intercept according to the burial history at depth. These information are crucial to the interpretation of the geology and seismic outcome in the search for hydrocarbons. In this study we loaded in Yttergryta and Natalia well log data in PeLe, and we get result visualizations from different scenarios for each of them in PeLe.

5.2.1 PeLe-results from Yttergryta

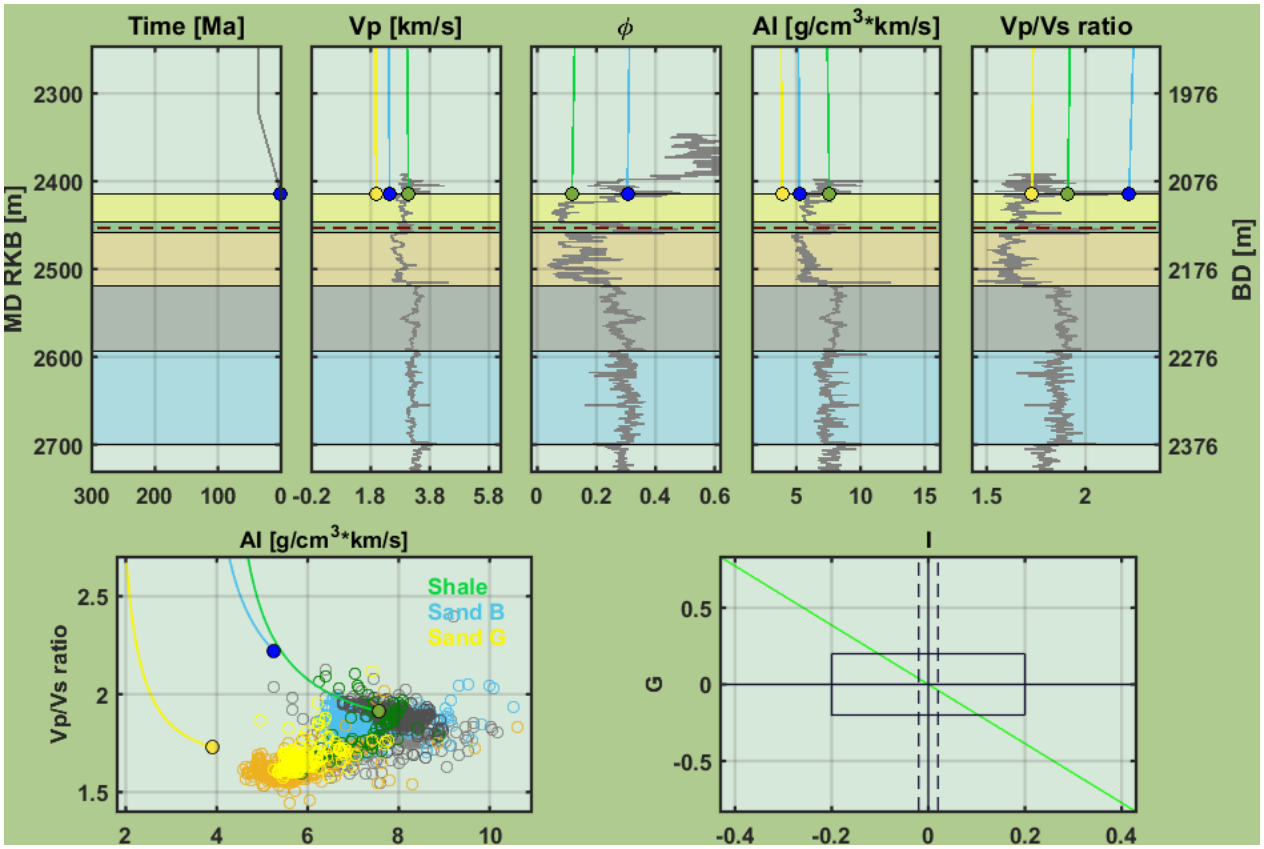

Figure 20: PeLe-modeling at temperature 31 Celsius at Yttergryta

Figure 20 shows the seismic responses from Garn Fm to Tilje Fm at temperature 31 Celsius at Yttergryta. The burial sequence was rapid, and it didn't reach the cementation process. That we can see by the dotted brown line across the first five graphs at Figure 20, and this is called the cementation line. The light blue line is water-sand, yellow line is gas and the green line is shale on Figure 20. The circled dots is the position for today's level on Figure 20. At the graph of V_p/V_s ratio versus AI, we can see that yellow gas line and light blue water-sand line doesn't hit the circled area meant for them at Yttergryta.

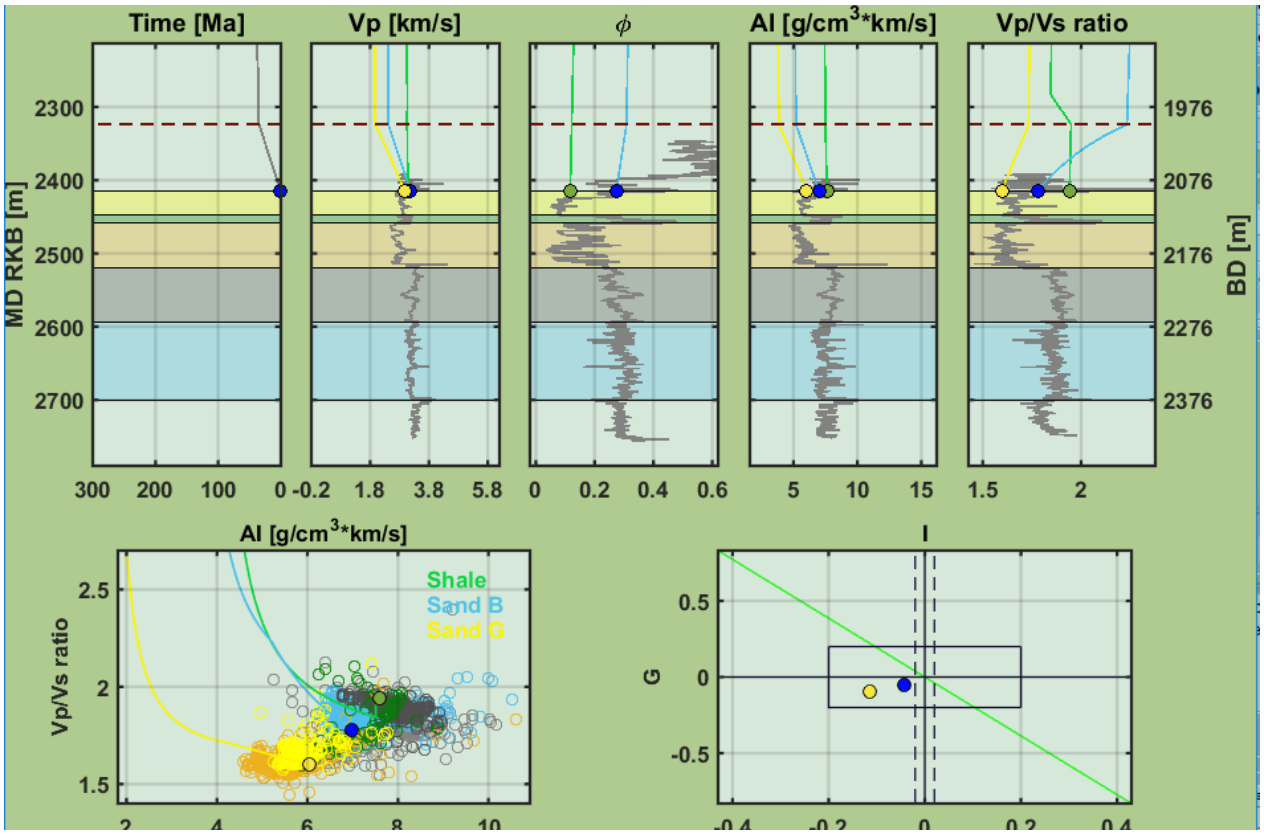

Figure 21: PeLe-modeling at temperature 33 Celsius at Yttergryta

Figure 21 shows the burial sequence is steady downwards, and when it hits the cementation line one can see that the burial sequence gets faster towards to today's level. That's because the chemical compaction occurs and the porosity decreases, such that the mechanical and chemical compaction boost the burial sequence to today's level. The graph of V_p/V_s ratio versus AI on Figure 21, we can see that yellow gas line and light blue water-sand line do hit the circled area meant for them at today's level. In addition, the graph of gradient versus intercept on Figure 21 shows the yellow gas dot and blue dot are in the AVO Class III. This coincides with the Figure 7 and Figure 8 from the theory section. It shows that the yellow gas dot is in the correct gas area and the blue dot is in the correct brine area. In addition, there is a separation between the yellow dot and blue for the oil area. This verifies that the gas and brine are in the correct area. We have to know that this scenario is done under assumption of boosted illite values, such that rock becomes a bit stiffer. Then it will be correct according to the graph of gradient versus intercept on Figure 21. We know from the geology section, that Garn Fm is gas-sand and Tilje Fm is water-sand.

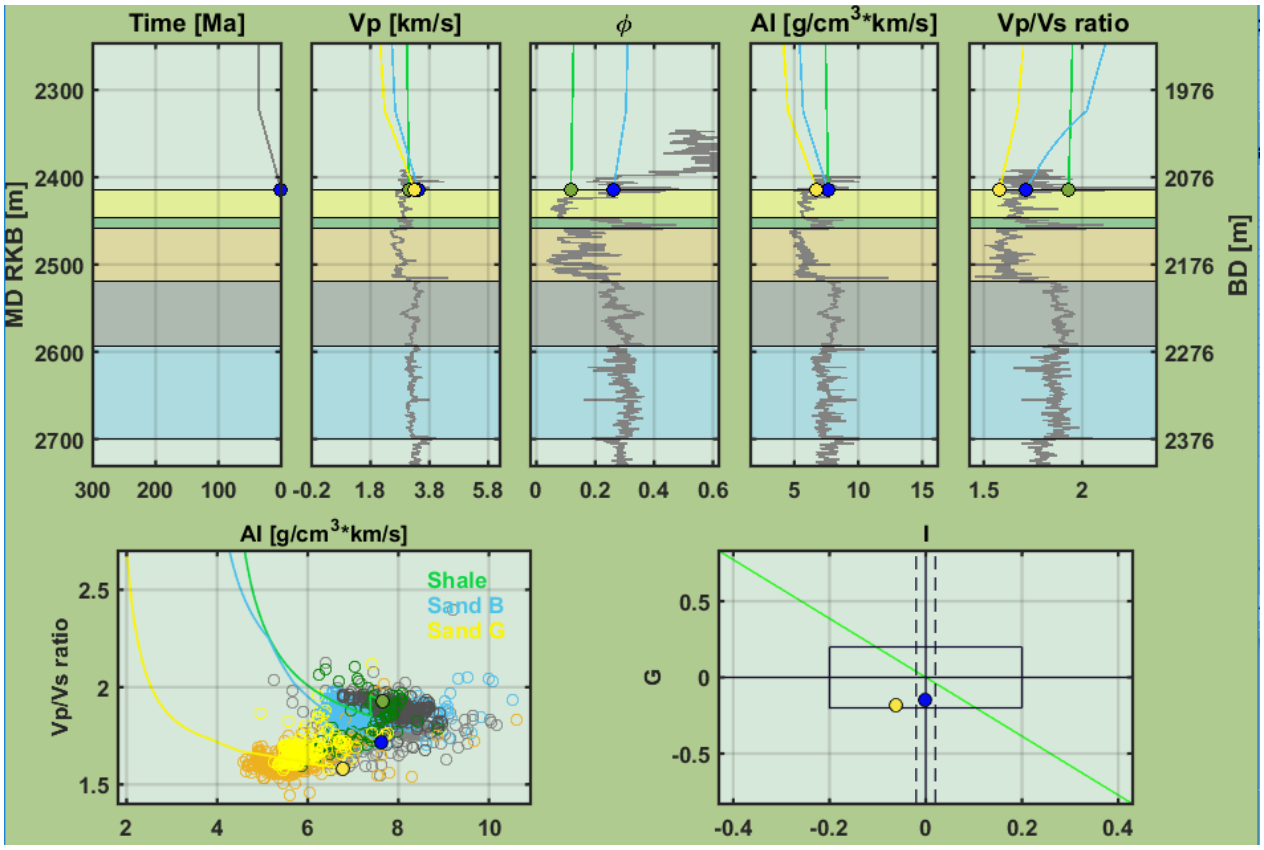

Figure 22: PeLe-modeling at temperature 35 Celsius at Yttergryta

Figure 22 shows the burial sequence is rapid towards today's level. The graph of V_p/V_s ratio versus AI on Figure 22 shows that yellow gas dot and blue brine dot goes past the area meant for them, unlike the scenario on 21. The graph of gradient versus intercept on Figure 22 shows the blue dot on AVO Class II at the intercept line and that's not fully correct for brine in a sand-based scenario. In addition, the yellow gas dot is wrongfully in the oil area.

Table 4: Values to Yttergryta after PeLe-modeling

Temp [c^0]	Layer	V_p [Km/s]	V_p/V_s	V_s [Km/s]	Rho[g/cm^3]
31	Brine sand	2.44	2.21	1.10	2.15
31	Shale	3.02	1.90	1.59	2.45
33	Brine sand	3.20	1.78	1.8	2.20
33	Shale	3.20	1.93	1.65	2.46
35	Brine sand	3.43	1.71	2.00	2.23
35	Shale	3.11	1.93	1.60	2.47

The seismic parameters from Table 4 is used in DigAVO, where they are used to get the training data by Monte Carlo-simulation in a stage to generate the AVO-classification of facies/fluids to Yttergryta.

5.2.2 PeLe-results from Natalia

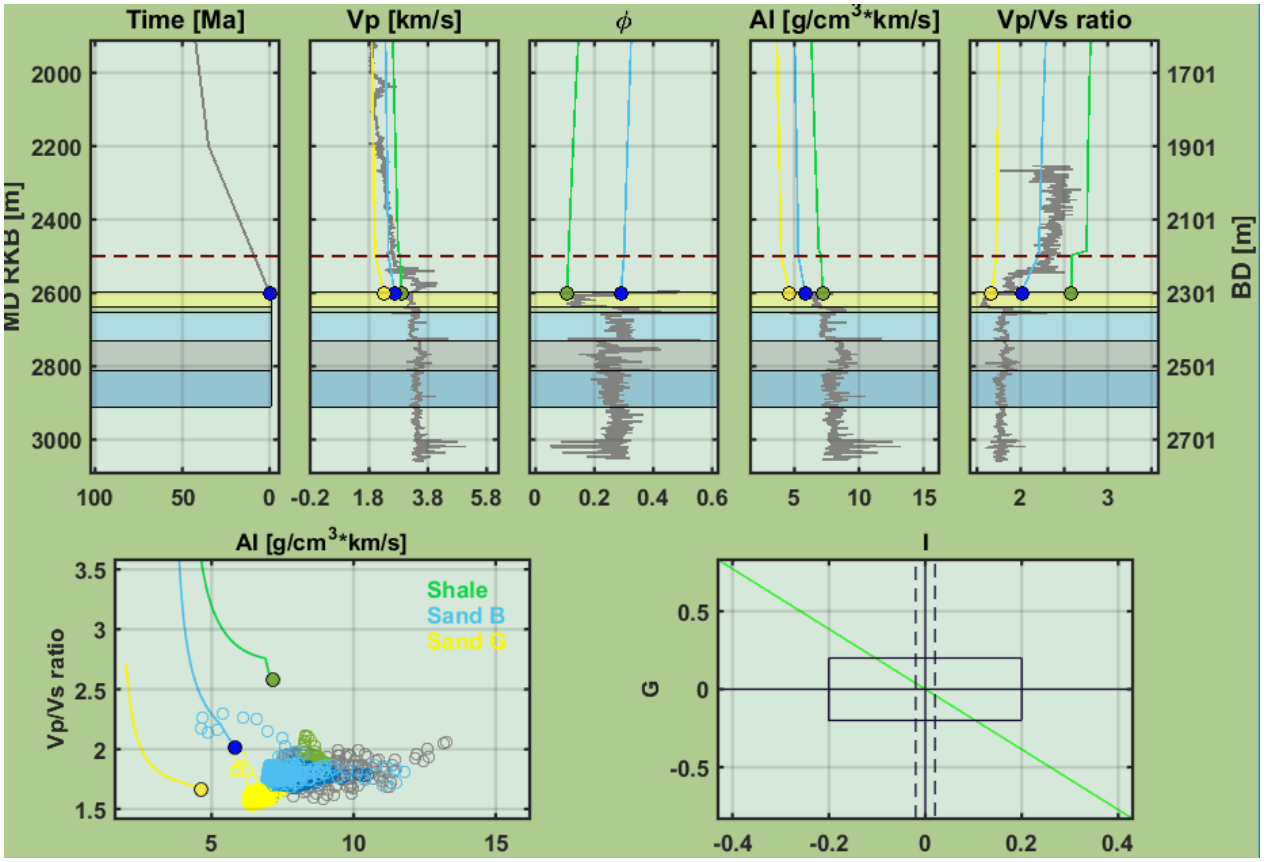

Figure 23: PeLe-modeling at temperature 30 Celsius at Natalia

Figure 23 shows the seismic responses from Garn Fm to Tilje Fm at temperature 30 Celsius at Natalia. It shows the burial sequence steady to 2200 meters and then it goes faster towards today's level. We can make a note that cementation line didn't have a significant at the end of the burial sequence. The graph of V_p/V_s ratio versus AI on Figure 23 shows that yellow gas dot and blue brine dot doesn't reach the area meant for them.

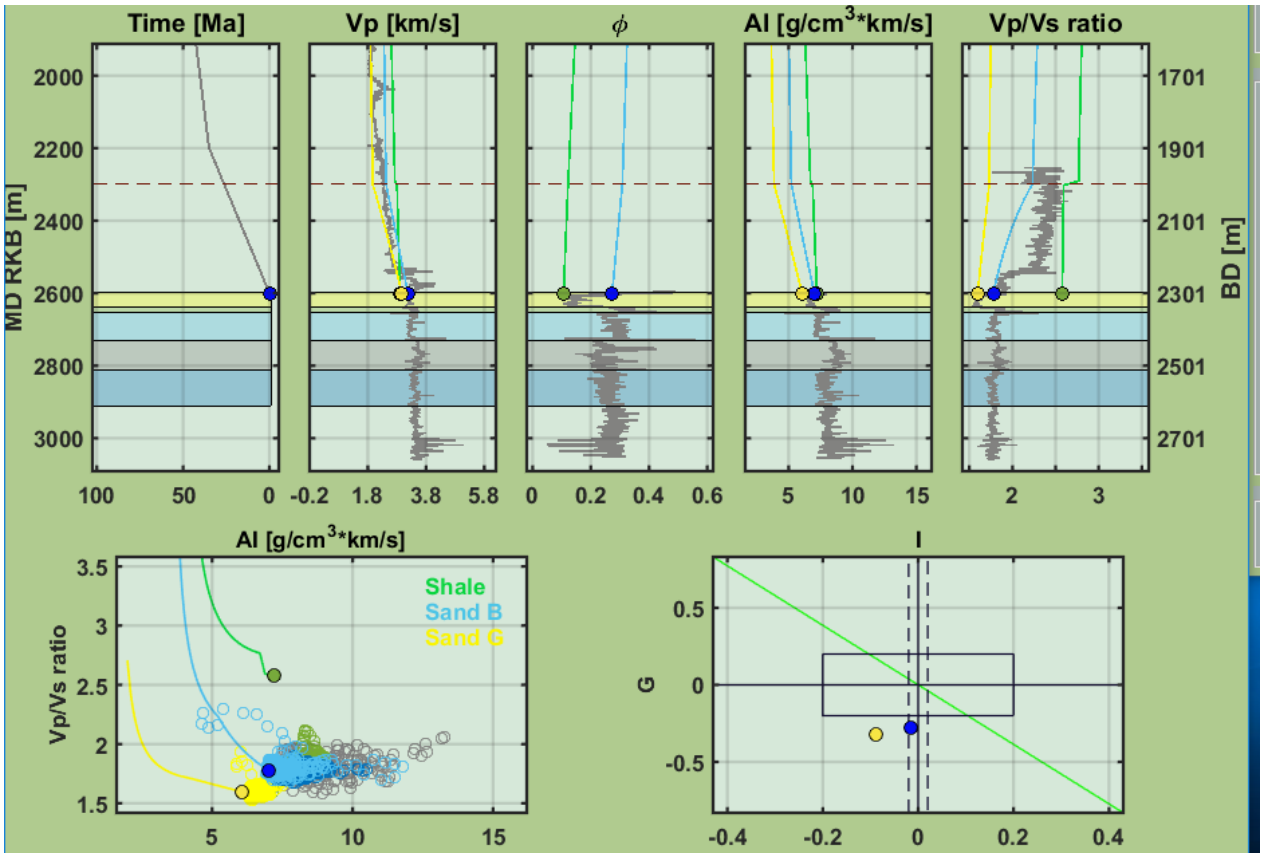

Figure 24: PeLe-modeling at temperature 34 Celsius at Natalia

Figure 24 shows the burial sequence steady to 2200 meters. Then it goes faster well before the cementation line and towards today's level. The graph of V_p/V_s ratio versus AI on Figure 24 indicates that yellow gas dot and blue brine dot reach slightly the area meant for them. In PeLe-modeling for Natalia didn't we use the assumption of boosted illite values, such that we could ha the possibility of the rocks to stiffer. Thereby can we showcase the effect of the shale has on AVO-classes and on the graph of gradient versus intercept on Figure 24. Thereby, we should in PeLe-modeling for Natalia look beside the graphs of gradient versus intercept on all figures in Natalia section here.

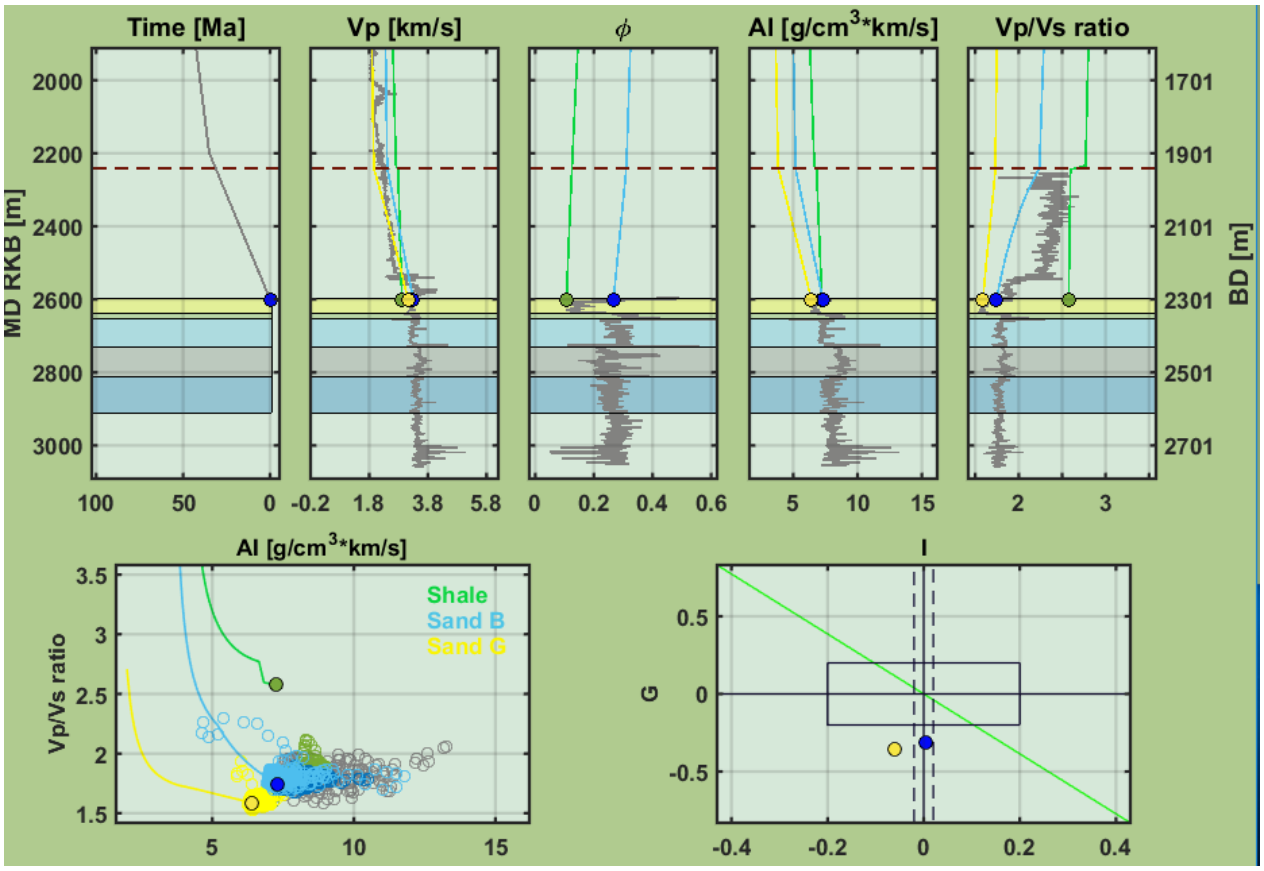

Figure 25: PeLe-modeling at temperature 35 Celsius at Natalia

Here on Figure 25 we can make comparison to Figure 24 with that we just increases the temperature with one degrees. Figure 25 one can see that the cementation has bigger impact than on Figure 24 by that the burial sequence goes increasingly faster towards to today's level after passing the cementation line. In addition, we can see the graph of V_p/V_s ratio versus AI on Figure 25 indicates that yellow gas dot and blue brine dot reach more the indicated area meant for them compared to the graph of V_p/V_s ratio versus AI on Figure 24. From the geology section we know that Garn Fm is gas-sand and Tilje Fm is water-sand in Natalia. All these information gives more accuracy that the intended scenario did likely happened than the scenario on Figure 24, and the result on Figure 25 indicates that the temperature is most truly correct for Natalia.

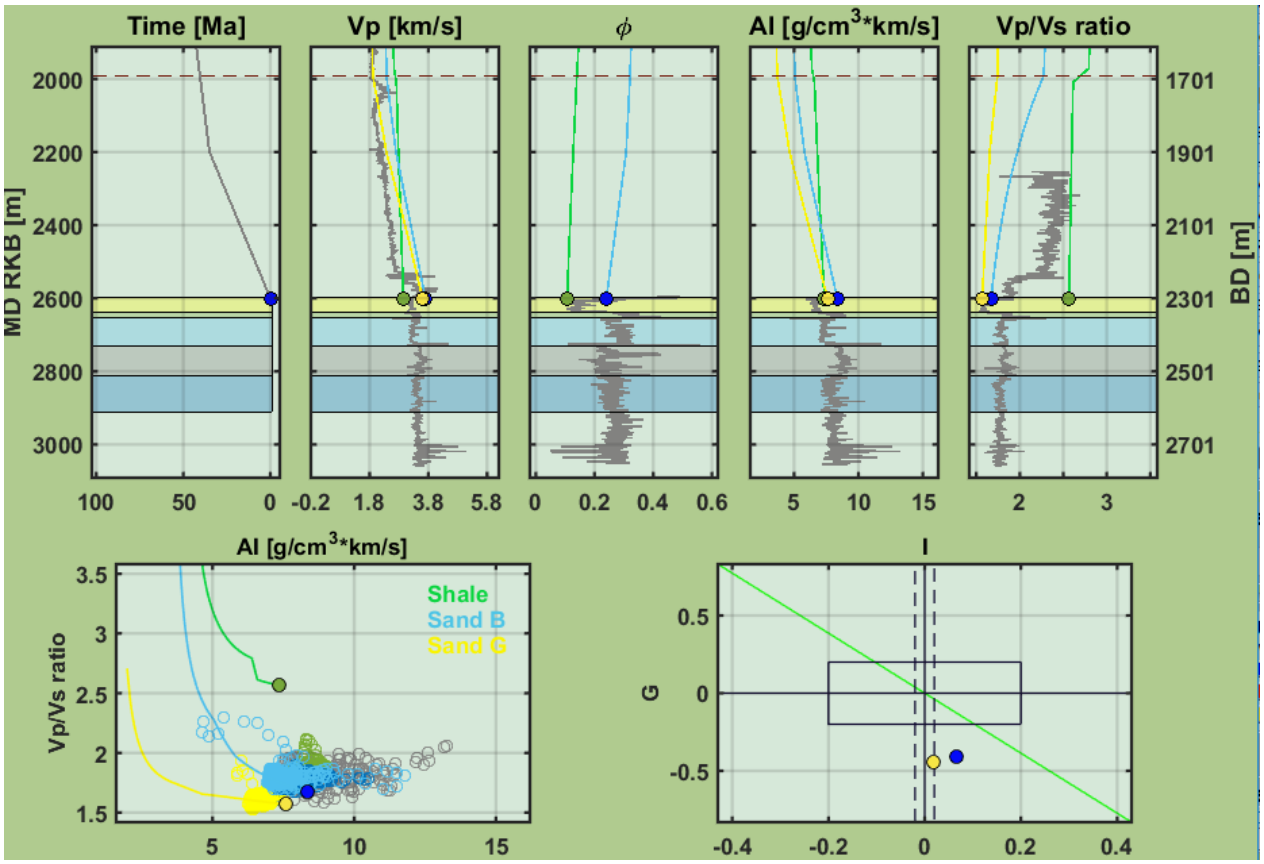

Figure 26: PeLe-modeling at temperature 39 Celsius at Natalia

In this last part of PeLe-modeling we wanted to see if we increased the temperature with five degrees to see the effects. Figure 26 one can see the cementation line is way high up compared to the other graphs in Natalia. The burial sequence has been affect a bit by the cementation, but not rapid affect towards to today's level. We can see on the graph of V_p/V_s ratio versus AI on Figure 26 that yellow gas dot and blue brine dot goes past the area suited for them.

Table 5: Values to Natalia after PeLe-modeling

Temp [c^0]	Layer	V_p [Km/s]	V_p/V_s	V_s [Km/s]	Rho[g/cm^3]
30	Brine sand	2.68	2.02	1.33	2.17
30	Shale	2.82	2.56	1.10	2.48
34	Brine sand	3.18	1.70	1.83	2.20
34	Shale	2.81	2.52	1.18	2.50
35	Brine sand	3.22	1.74	1.85	2.21
35	Shale	2.86	2.56	1.20	2.51
39	Brine sand	3.69	1.68	2.20	2.25
39	Shale	2.95	2.56	1.15	2.48

The seismic parameters from Table 5 is used in DigAVO. They are used to get the training data by Monte Carlo-simulation in a stage to generate the AVO-classification of facies/fluids to Natalia.

5.3 DigAVO

The results from DigAVO are the final results visualization after using the outputs from Hampson Russell AVO and PeLe. Here we will see Litho/Fluid classification of the well locations. In addition, to see which temperature choices provide the most accurate range in well locations, and are there potential traps / anomalies that reveal shallower or deeper, better seen at some other temperatures.

5.3.1 DigAVO results for xline 2508 Yttergryta

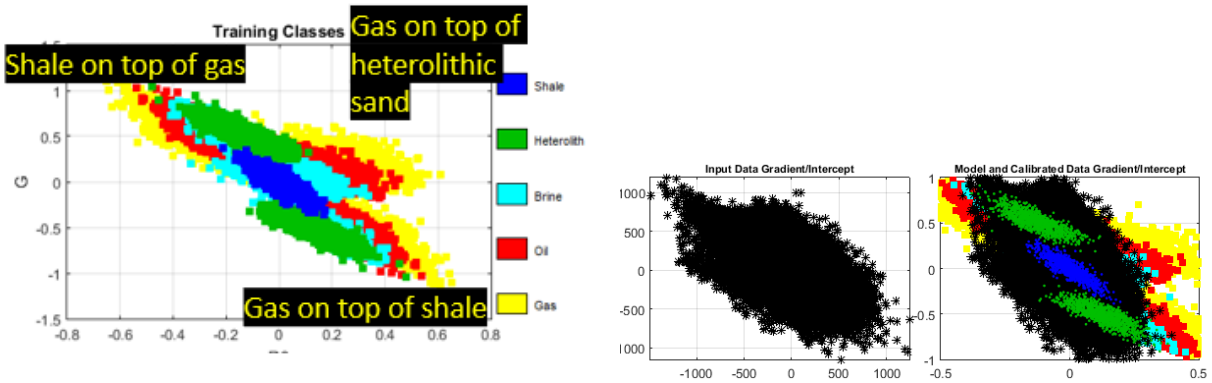

(a) Training classes for xline 2508 Yttergryta at temperature 31 Celsius

(b) The calibration for xline 2508 Yttergryta at temperature 31 Celsius

Figure 27: The results from calibration for xline 2508 Yttergryta at temperature 31 Celsius

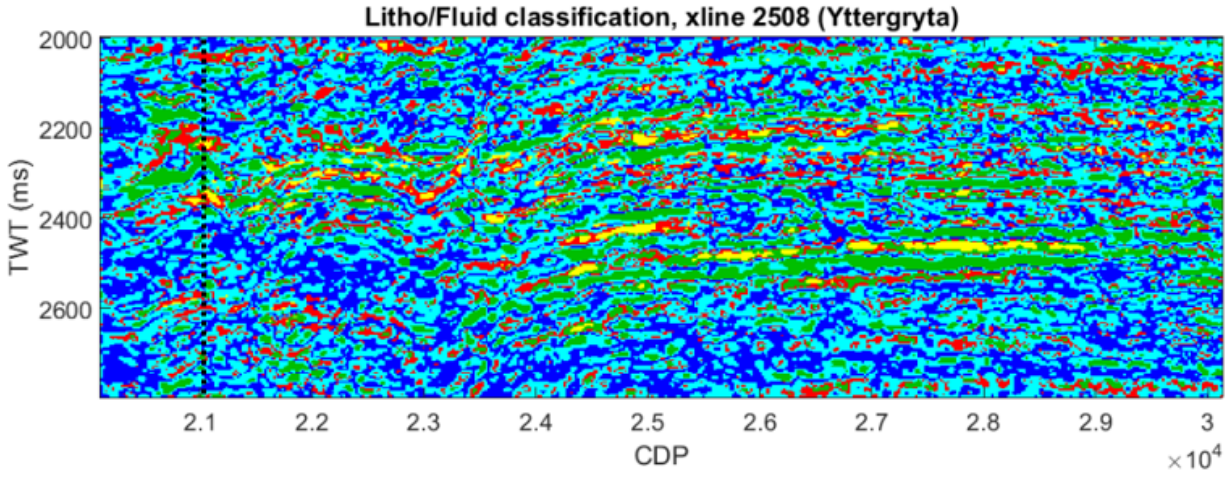

Figure 28: Litho/Fluid classification, xline 2508 Yttergryta at 31 Celsius

Xline 2508 Yttergryta at temperature 31 Celsius shows on the classification on Figure 28 that it isn't very realistic. There are too much sand in the Cretaceous on Figure 28, and it's unconsolidated sand at this temperature. The calibration on Figure 27*b* doesn't fit well either. This classification gives not the right picture of the well location.

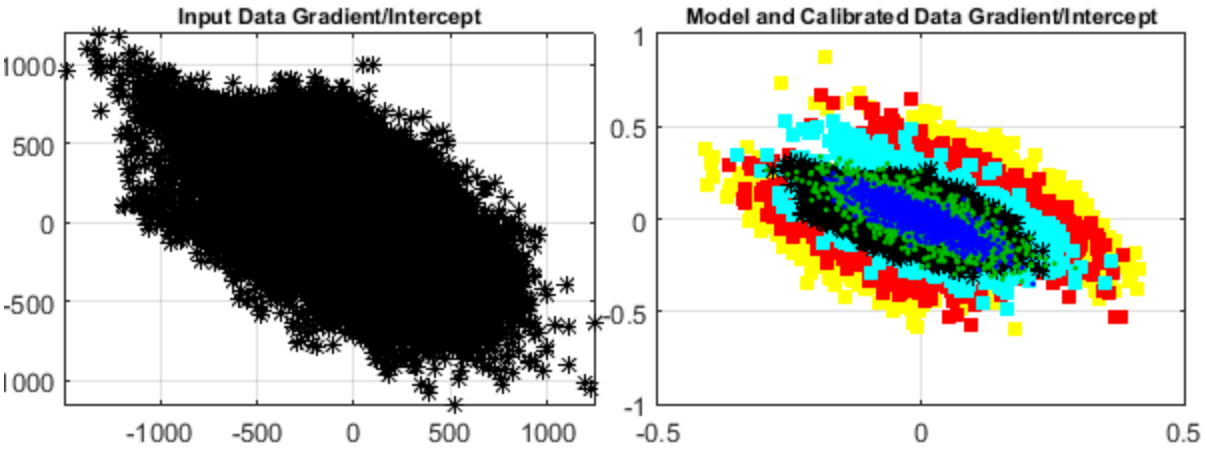

Figure 29: The results from calibration for xline 2508 Yttergryta at temperature 33 Celsius

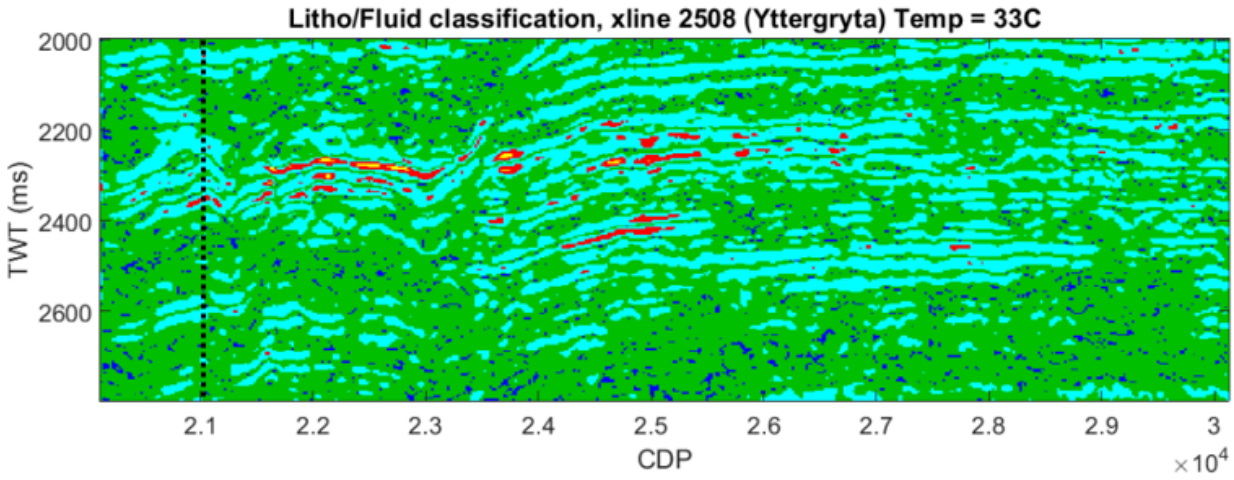

Figure 30: Litho/Fluid classification, xline 2508 Yttergryta at 33 Celsius

Figure 30 shows the classification a bit better than in Figure 28. But it doesn't catch up shale on the black line at Yttergryta on Figure 30. Most of it becomes sand or heterolith, but the flat spot appears well in Yttergryta. The calibration a bit better than the last one, but this classification gives not the right range of the well location.

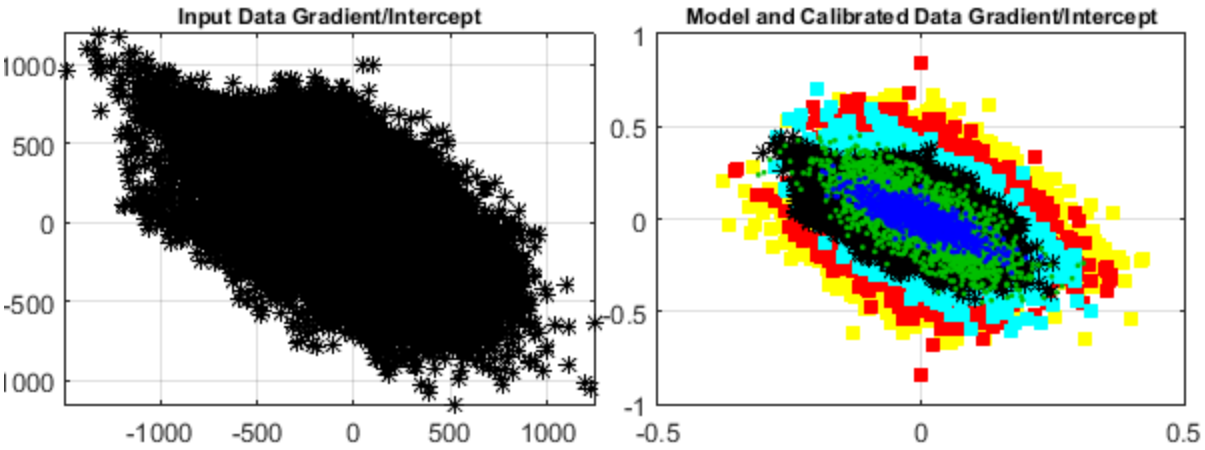

Figure 31: The results from calibration for xline 2508 Yttergryta at temperature 35 Celsius

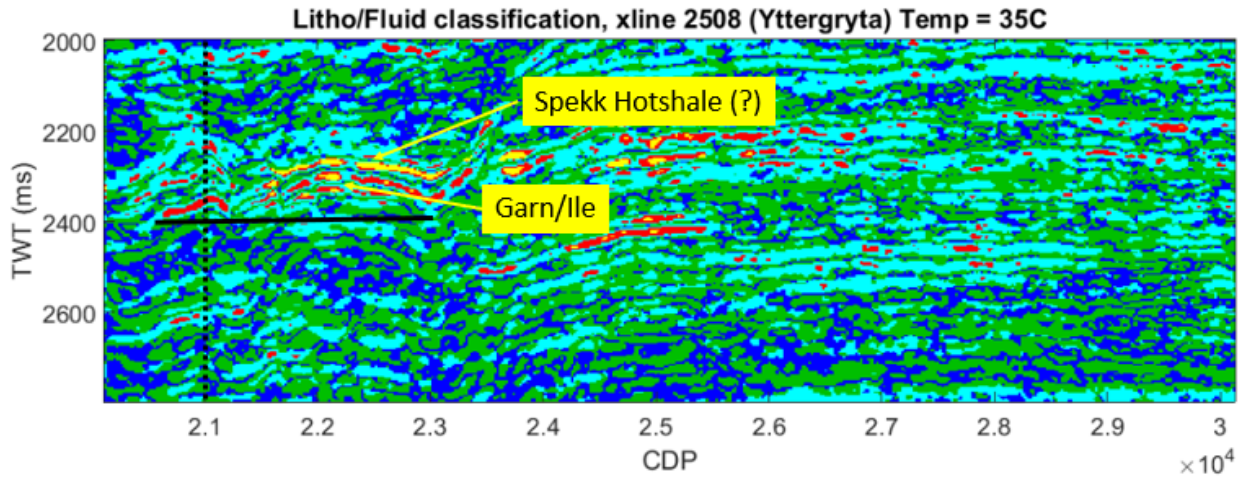

Figure 32: Litho/Fluid classification, xline 2508 Yttergryta at 35 Celsius

Figure 32 shows the shale in Cretaceous, Melke Fm and Ror Fm, and fluid contact is clearly seen in Yttergryta. One can see gas and gas condensate sandstones in Garn Fm and Ile Fm on Figure 32. We are unsure about the top yellow refletor is Upper Jura Rogn sand with hydrocarbons, or hot shale (Spekk Fm). Spekk Fm is very thin in well location, and we lack logs through it. The calibration on Figure 31 fits well. This classification on Yttergryta at temperature 35 Celsius gives a very good picture of the actual well location.

5.3.2 DigAVO results for inline 2096 Yttergryta

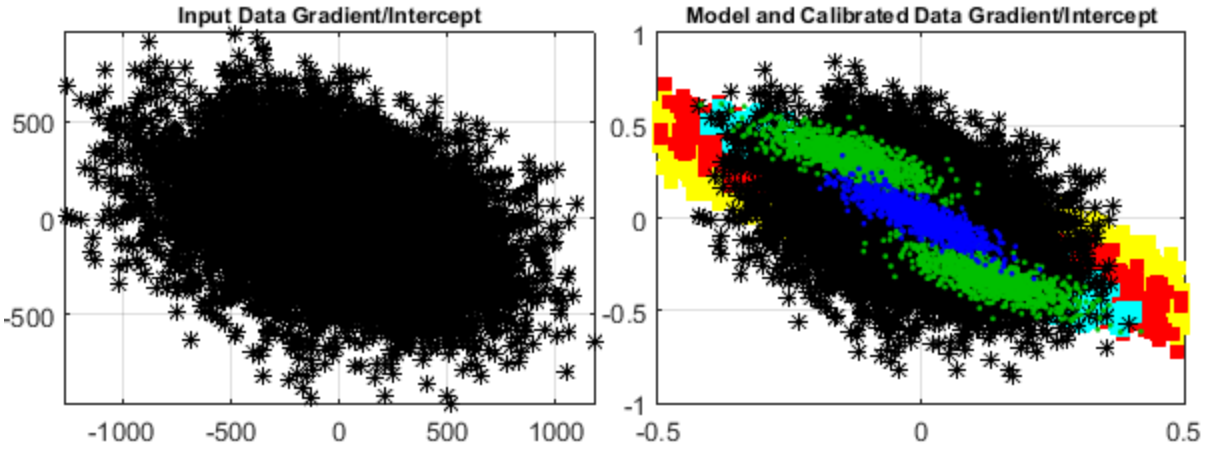

Figure 33: The results from calibration for inline 2096 Yttergryta at temperature 31 Celsius

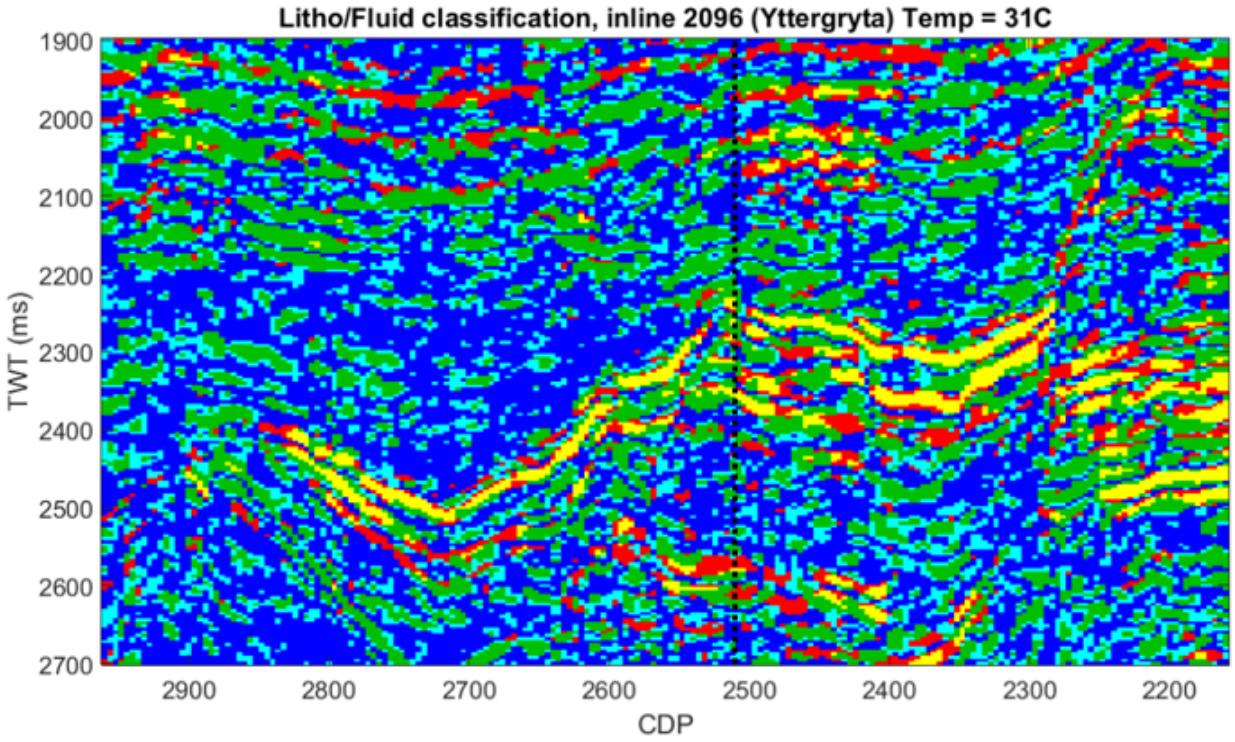

Figure 34: Litho/Fluid classification, inline 2096 Yttergryta at 31 Celsius

Figure 34 shows the classification at the inline 2096 Yttergryta at temperature 31 Celsius. It's not very realistic classification, because there are too much sand in Cretaceous. The calibration on Figure 33 is very bad, and it doesn't fit. This classification gives not the right picture of the well location.

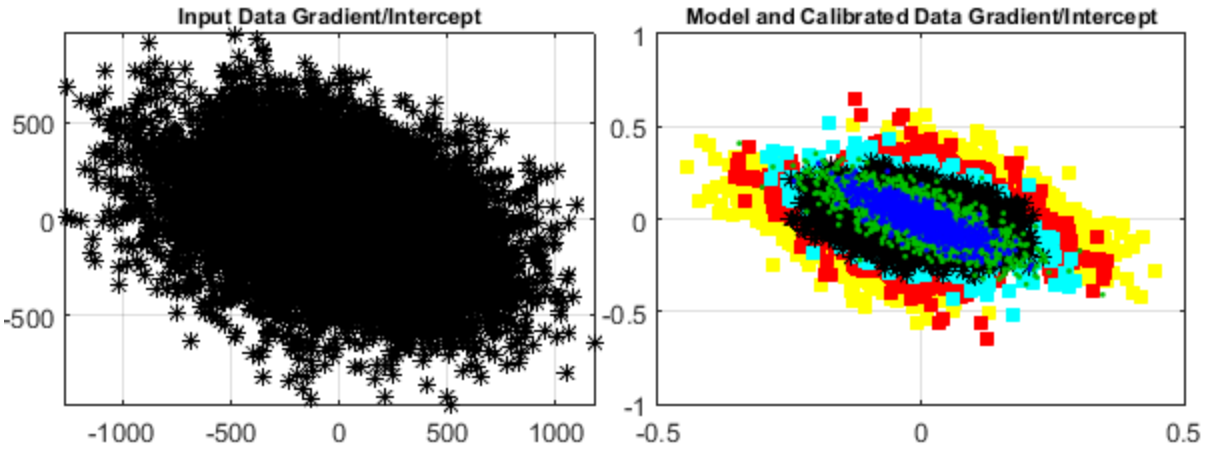

Figure 35: The results from calibration for inline 2096 Yttergryta at temperature 33 Celsius

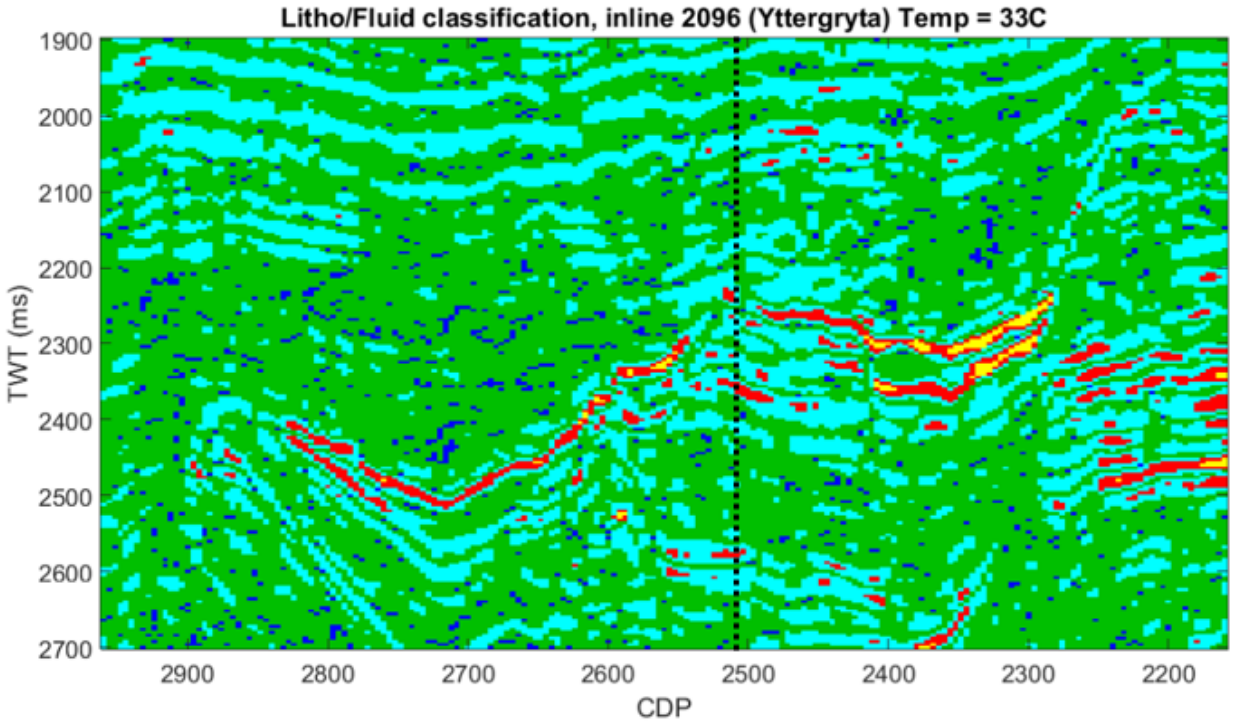

Figure 36: Litho/Fluid classification, inline 2096 Yttergryta at 33 Celsius

In comparison between Figure 36 and Figure 34, shows the classification a little better in Figure 36. But it doesn't catch up the shale, and most of it becomes sand or heterolith. The red flat spot appears well in Yttergryta. The calibration on Figure 35 fits better as well, but this classification at temperature 33 Celsius gives not right range of the well location.

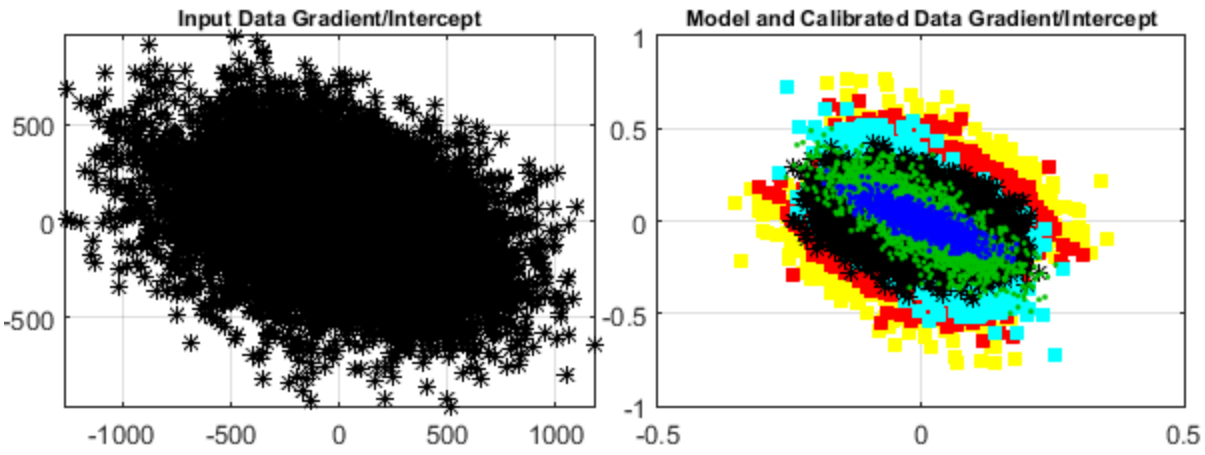

Figure 37: The results from calibration for inline 2096 Yttergryta at temperature 35 Celsius

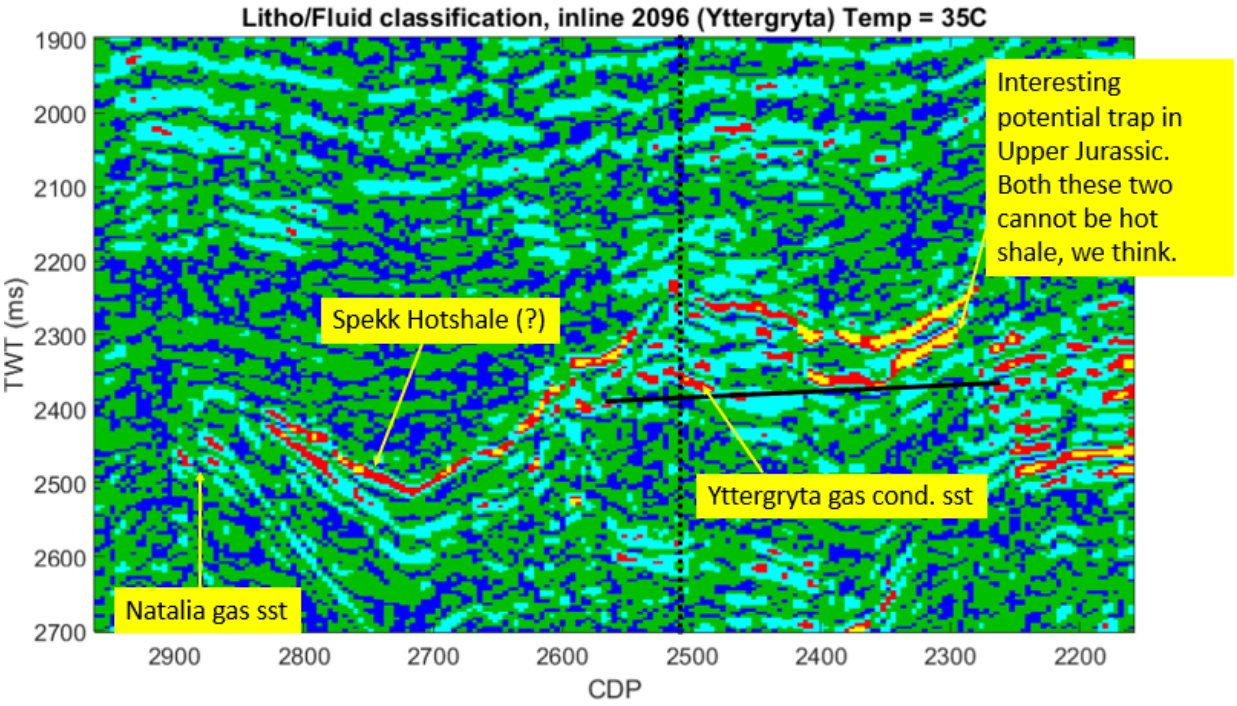

Figure 38: Litho/Fluid classification, inline 2096 Yttergryta at 35 Celsius

Figure 38 shows the Yttergryta gas condensate sandstones clearly. But condensate is almost like light oil. Furthermore, interpretation classification can be considered to be gas. For an example a more dirty sand with gas my look like oil filled in seismic. We think the Spekk Hotshale appears where the yellow arrow shows on Figure 38. There are an interesting potential trap in Upper Jurassic on the right side of Figure 38. We think that both these two cannot be hot shale. In addition, we can on the left side on Figure 38 see the Natalia gas sandstone appear, which we will explore more of in a later stage in this study. The calibration on Figure 38 fits well. This classification on inline 2096 Yttergryta at temperature 35 Celsius gives a very good picture of the well location.

5.3.3 DigAVO results for xline 2947 Natalia

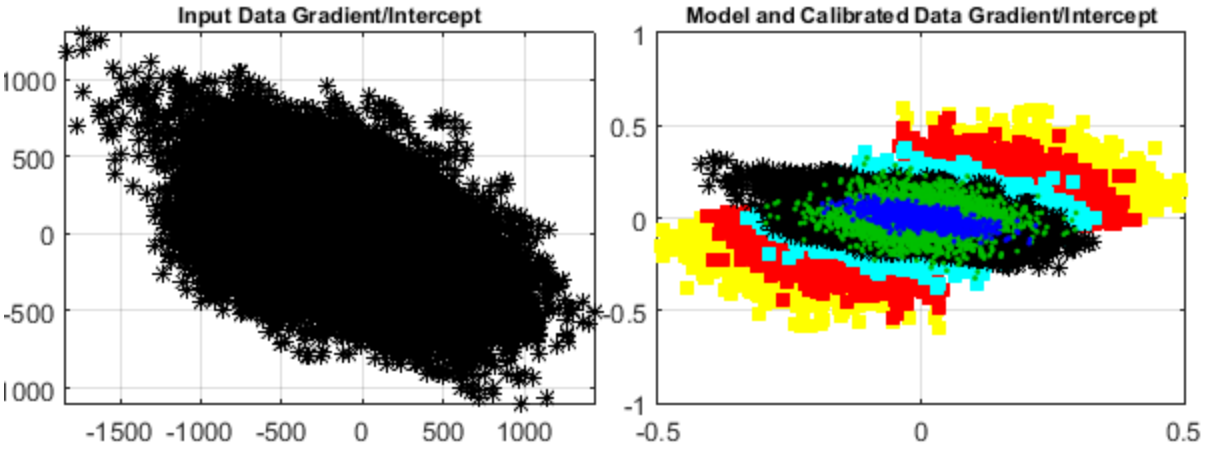

Figure 39: The results from calibration for xline 2947 Natalia at temperature 30 Celsius

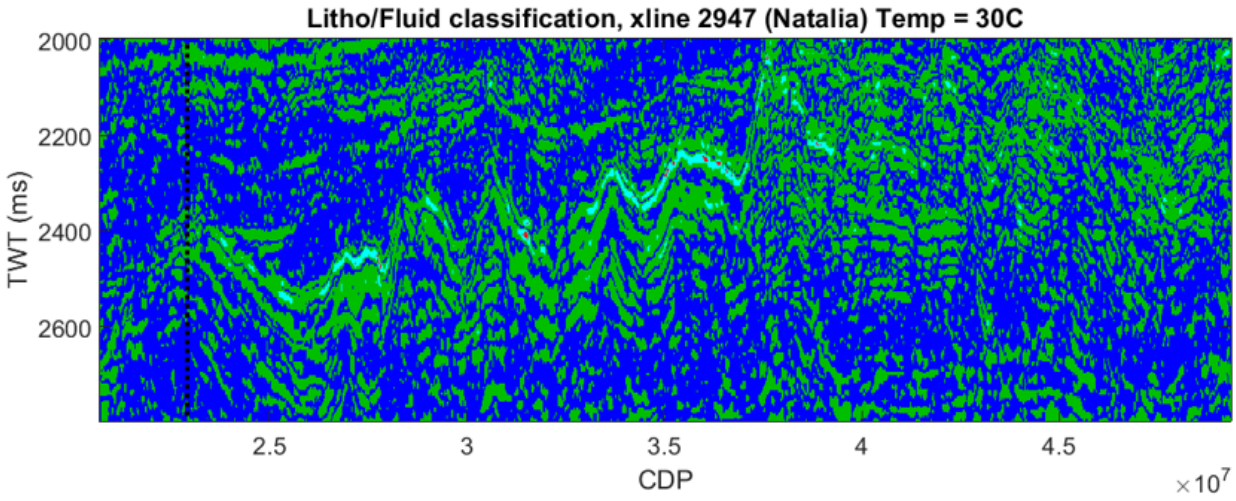

Figure 40: Litho/Fluid classification, xline 2947 Natalia at 30 Celsius

Figure 40 is dominated by shale and heterolith, and there are no hydrocarbon on the black line on Figure 40. The calibration on Figure 39 isn't good enough. This classification on xline 2947 Natalia at temperature 30 Celsius doesn't give a good picture of the well location.

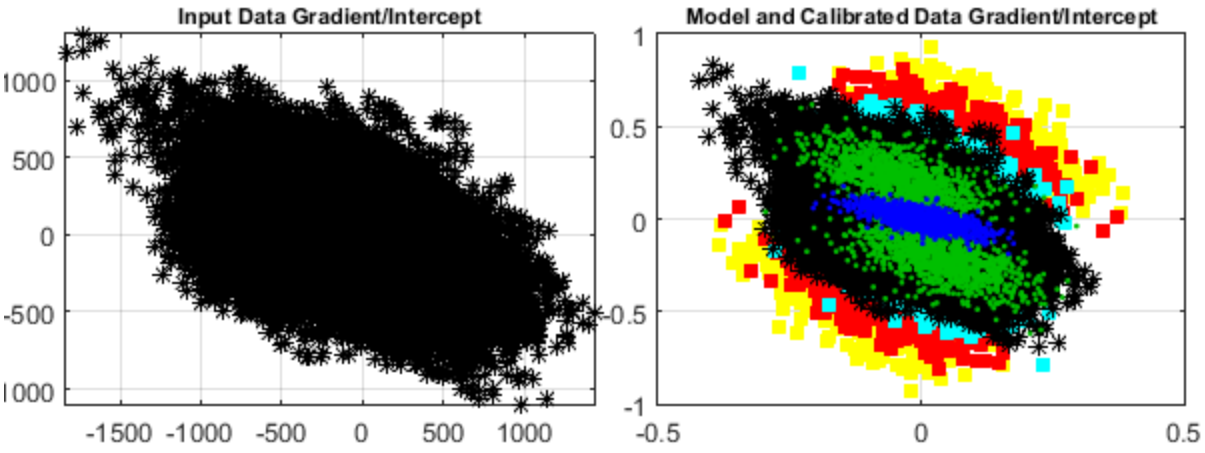

Figure 41: The results from calibration for xline 2947 Natalia at temperature 34 Celsius

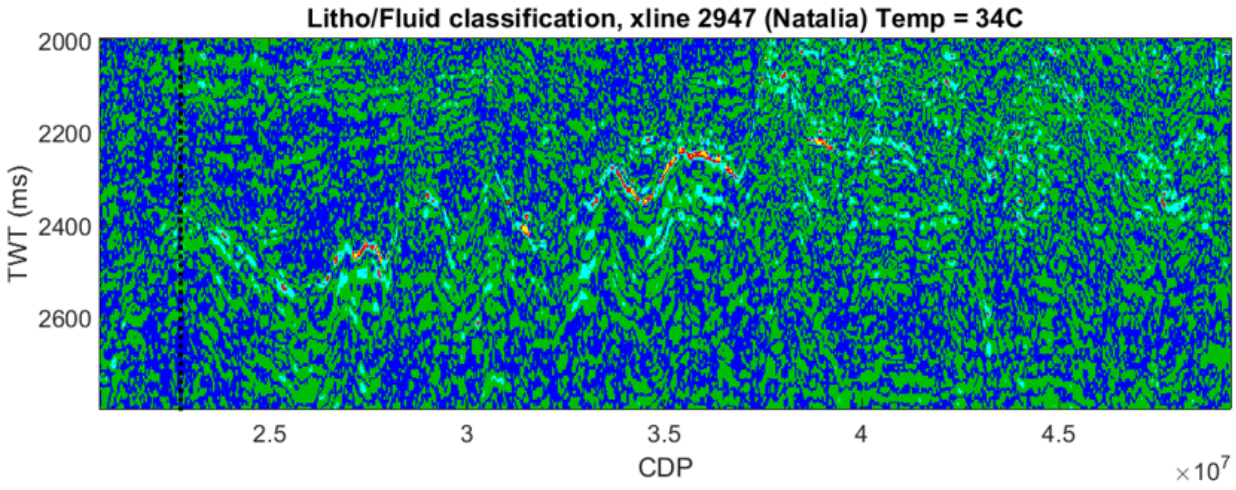

Figure 42: Litho/Fluid classification, xline 2947 Natalia at 34 Celsius

Figure 42 shows little better than Figure 40. But still dominated by shale and heterolith, and there are no hydrocarbons at the black line. There are no flat spot there. The calibration on Figure 41 doesn't fit very well. In addition, the structures doesn't appear good enough. This classification doesn't give a good range of the well location.

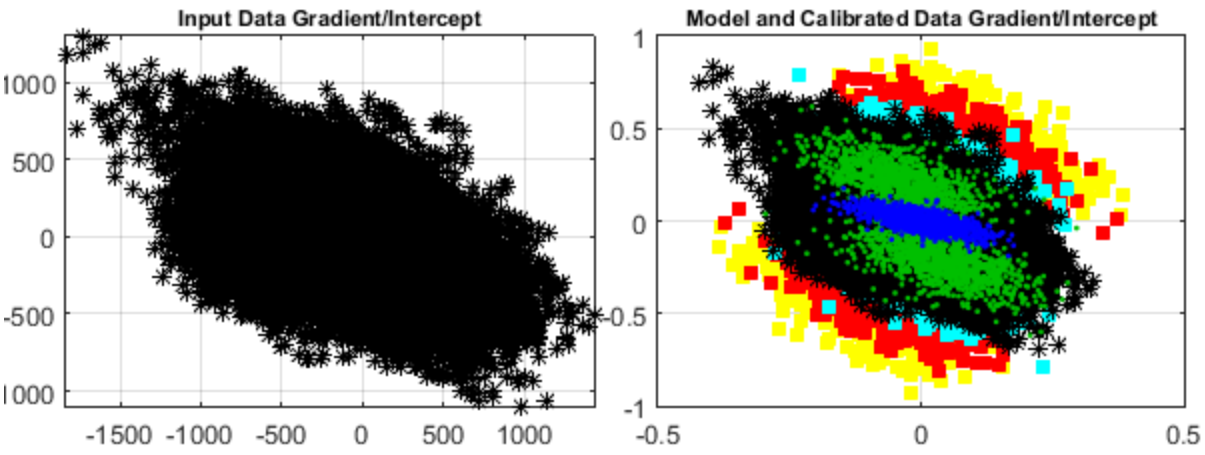

Figure 43: The results from calibration for xline 2947 Natalia at temperature 35 Celsius

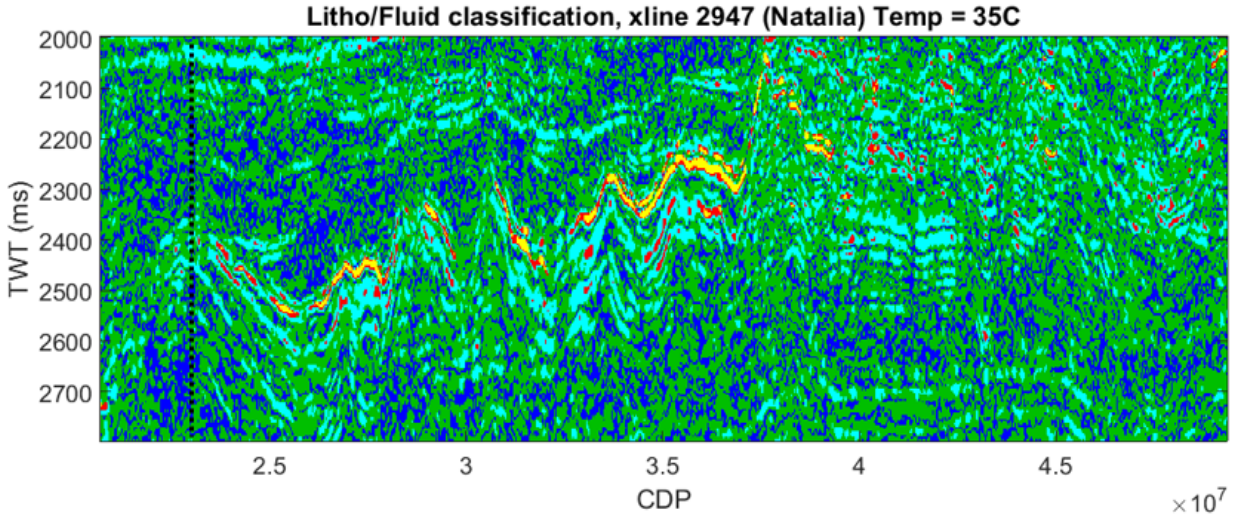

Figure 44: Litho/Fluid classification, xline 2947 Natalia at 35 Celsius

There are no hydrocarbons seen on the black line on Figure 44. This classification one can see that cementation plays a bigger in Natalia than Yttergryta. It's more cementation in Natalia. Thereby, it's more difficult to find the hydrocarbons.

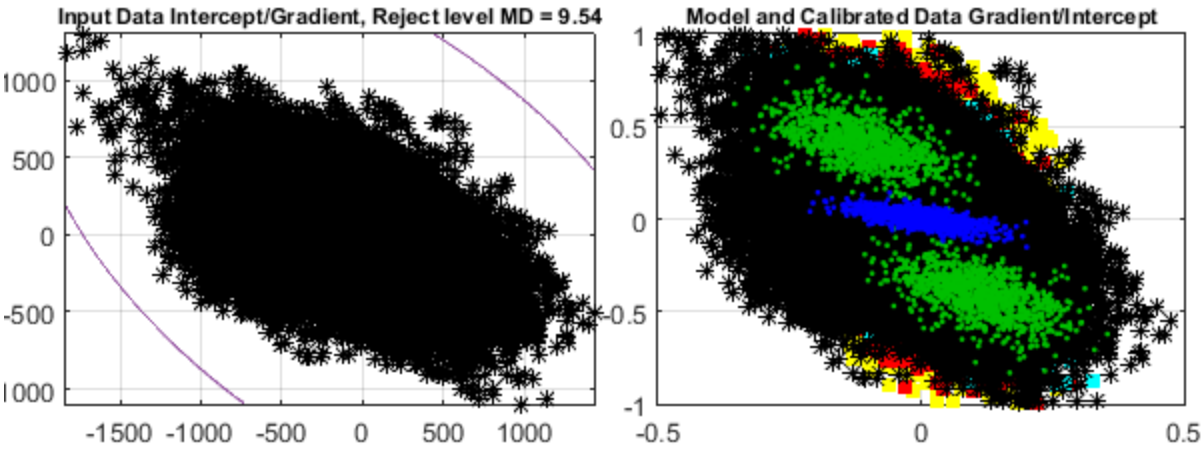

Figure 45: The results from calibration for xline 2947 Natalia at temperature 39 Celsius

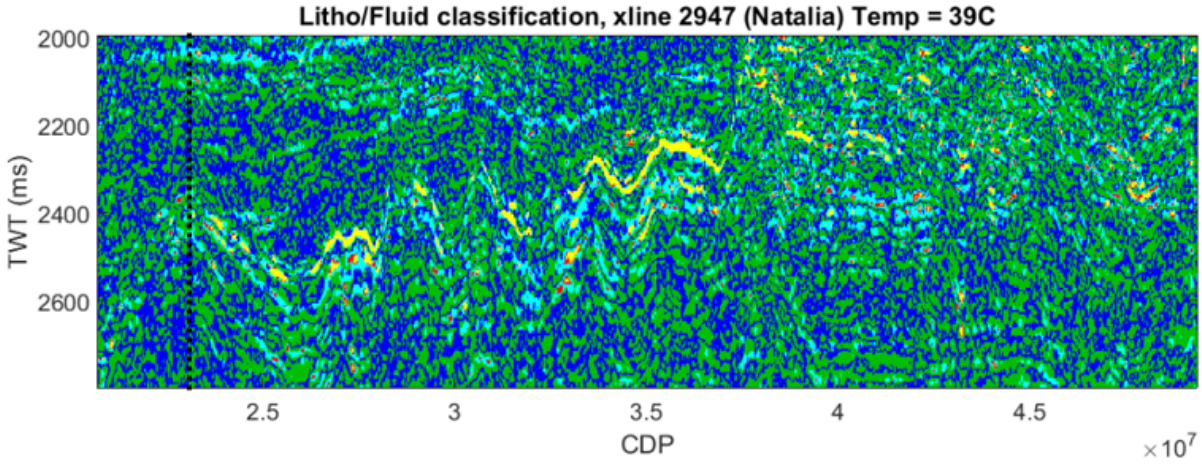

Figure 46: Litho/Fluid classification, xline 2947 Natalia at 39 Celsius

Figure 46 shows that it's dominated by heterolith and shale. There are very small hydrocarbon near the black line at Natalia. That is a possibility for gas in the Garn Fm there. But it's too much noise in the seismic to catch it. The cementation on Figure 46 is too much. Figure 45 shows the calibration doesn't fit at all, and this classification doesn't fit to well location at all.

5.3.4 DigAVO results for inline 2278 Natalia

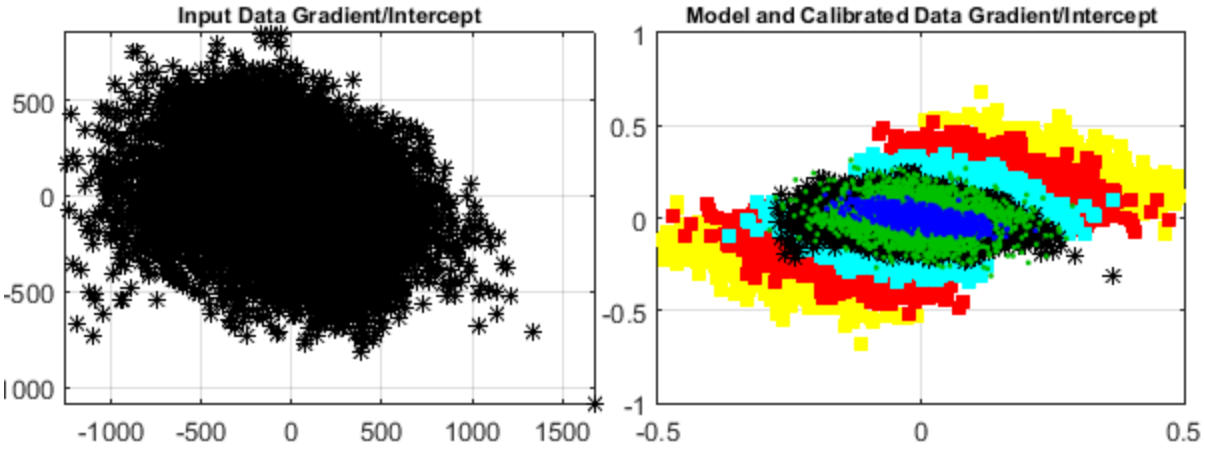

Figure 47: The results from calibration for inline 2278 Natalia at temperature 30 Celsius

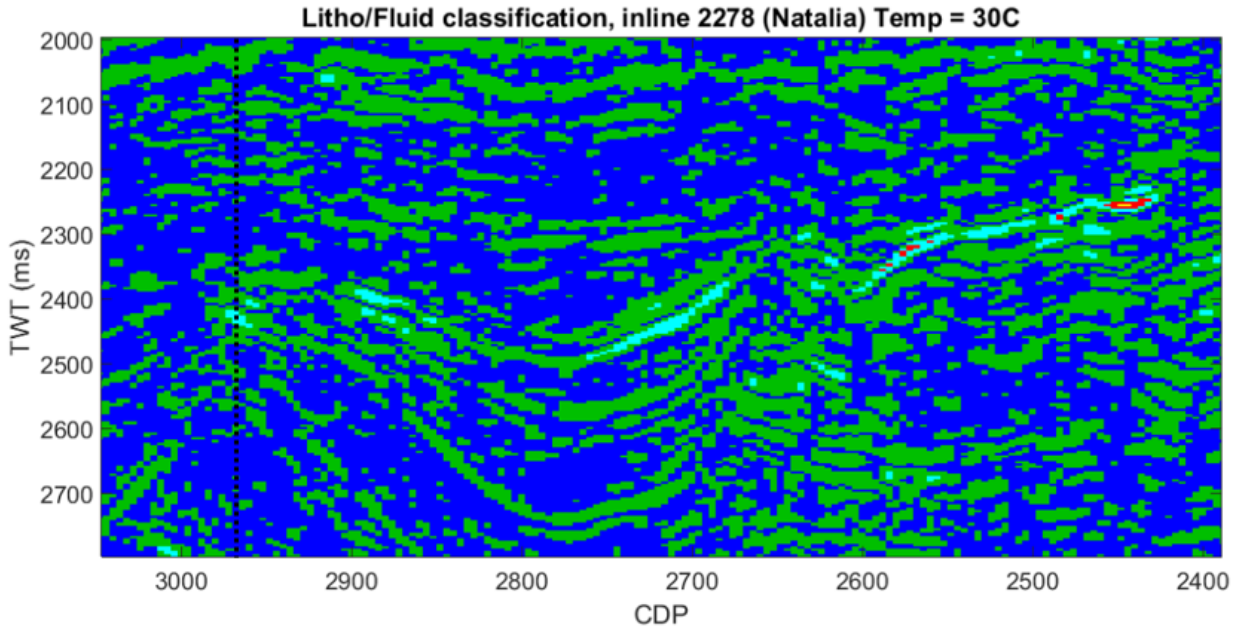

Figure 48: Litho/Fluid classification, inline 2278 Natalia at 30 Celsius

Figure 48 shows the classification on inline 2278 Natalia at 30 Celsius, where we on the black line on Figure 48 doesn't see hydrocarbons appear. It's dominated by shale and heterolith. This classification doesn't fit to well location.

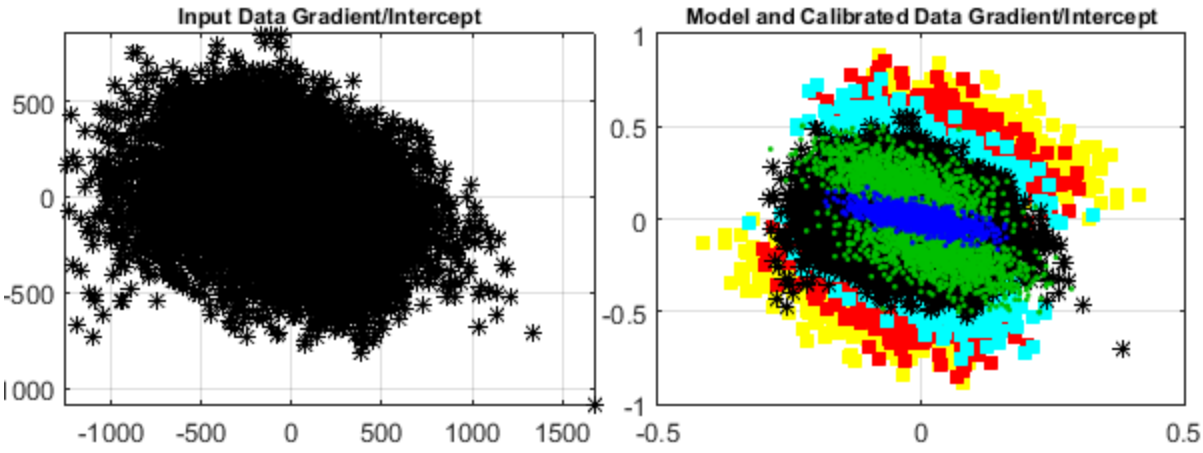

Figure 49: The results from calibration for inline 2278 Natalia at temperature 34 Celsius

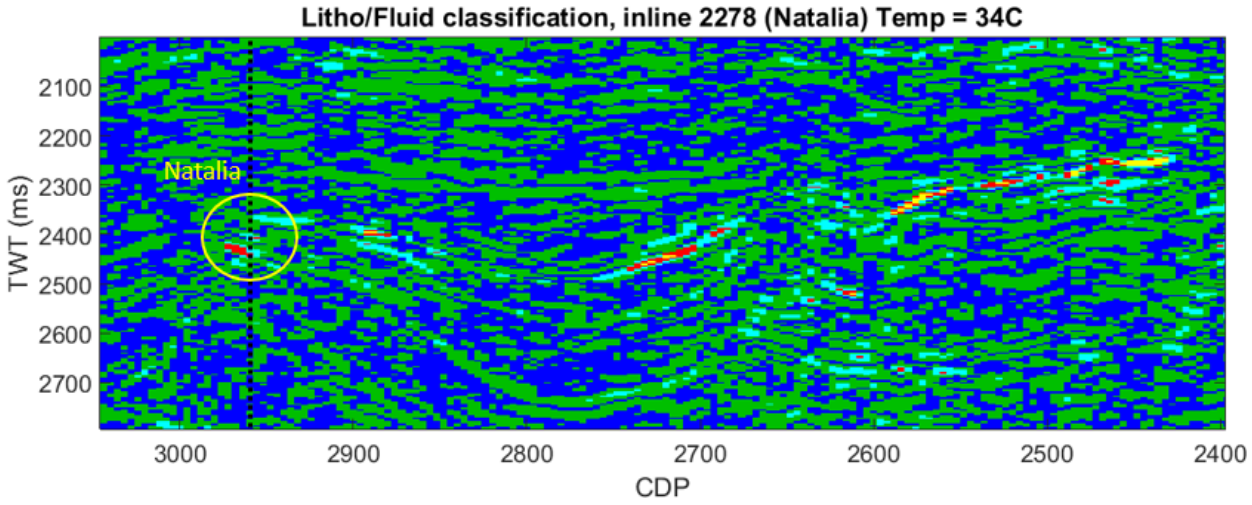

Figure 50: Litho/Fluid classification, inline 2278 Natalia at 34 Celsius

Figure 50 looks a bit better than Figure 48. We can see a little part of Natalia by the flat spot. But it's too much dominated by shale and heterolith, and this classification doesn't fit well with the well location.

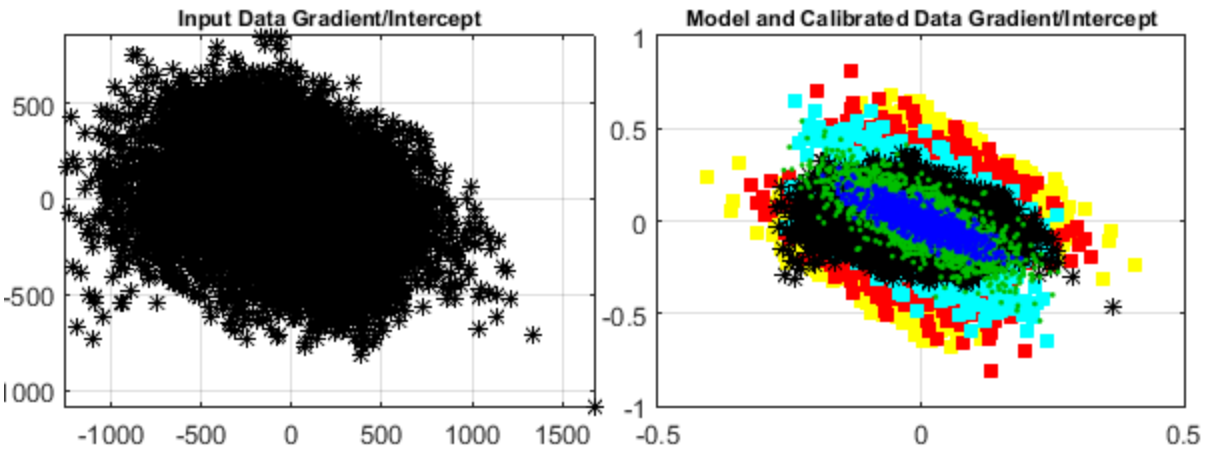

Figure 51: The results from calibration for inline 2278 Natalia at temperature 35 Celsius

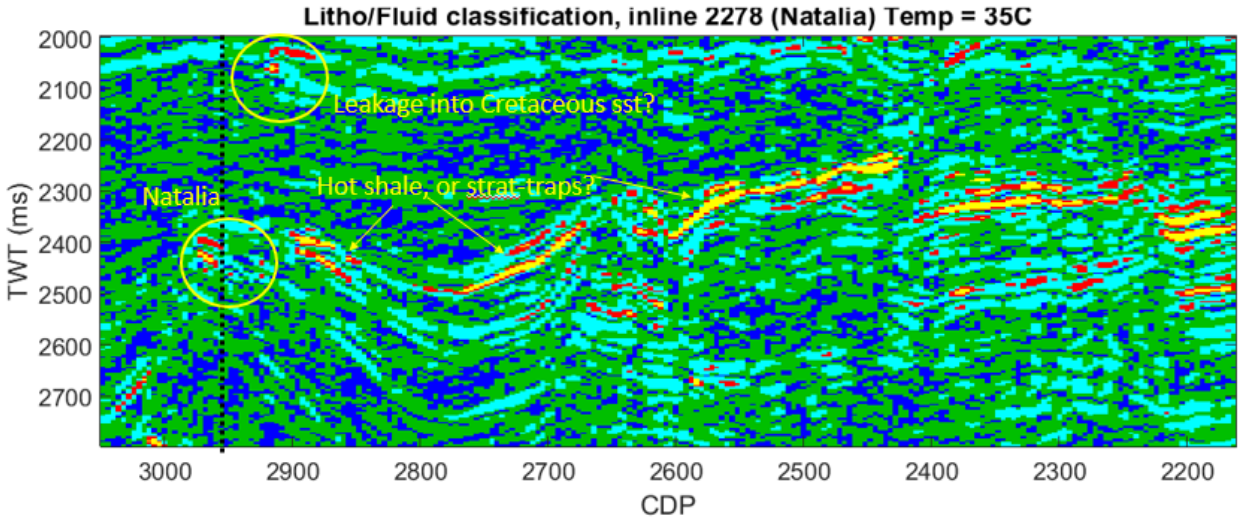

Figure 52: Litho/Fluid classification, inline 2278 Natalia at 35 Celsius

Figure 52 shows the fluid contact clearly in Natalia. We can possible see a hydrocarbon leakage from Natalia and into the Cretaceous sandstones, which are shown on the top of Figure 52. We are unsure about the hot shale on Figure 52 because of its thin thickness. But we think there are hot shale or stratigrafic traps that are shown by three yellow arrows on Figure 52. The calibration on Figure 51 fits well. This classification on inline 2278 Natalia at temperature 35 Celsius gives a very good picture of the well location.

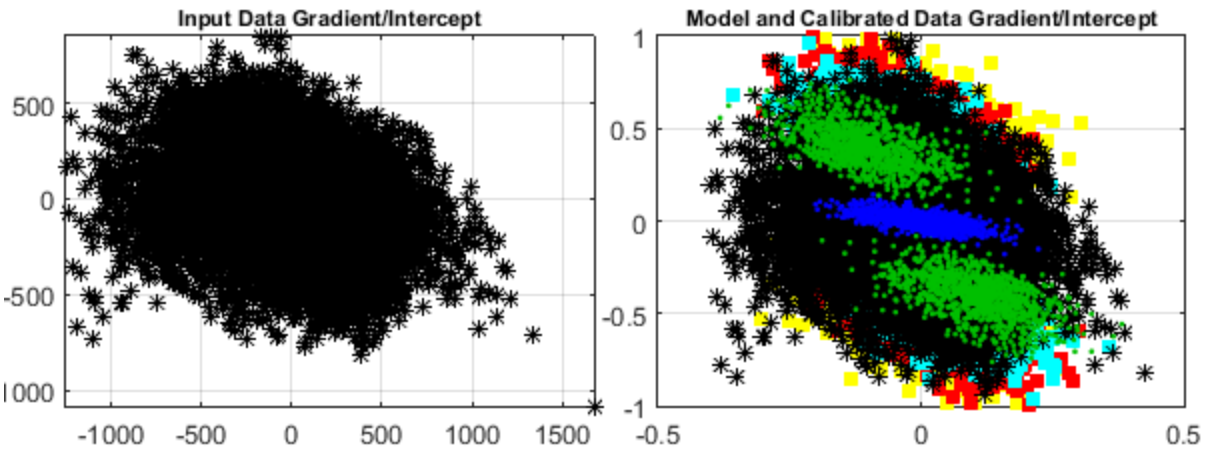

Figure 53: The results from calibration for inline 2278 Natalia at temperature 39 Celsius

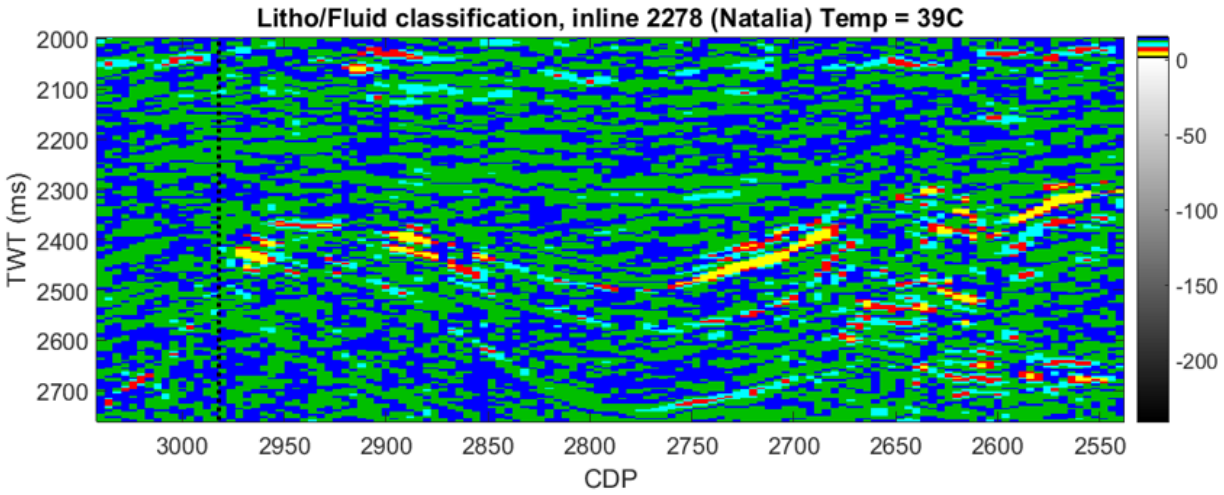

Figure 54: Litho/Fluid classification, inline 2278 Natalia at 39 Celsius

This classification on 54 isn't realistic. There are too much cementation and we can't see the the structures at all. There are no hydrocarbons seen on the black line on Figure 54. Figure 53 shows the calibration doesn't fit at all. This classification gives no range of the actual well location.

6 Discussion

In this study we applied a stiffer shale in the Yttergryta case in PeLe, which is more realistic. We boosted the shale values such that we "hacked" the mineralogy characteristic to fit the shale for Melke Fm in the well data. There we had V_p/V_s to around 1.8-1.9. In the PeLe-results for the right temperature 35 Celsius, we got the correct picture of the well location for Natalia. But it was slightly incorrect for Yttergryta, which can do with the boosted shale values. There can be a possibility that we boosted slightly with a wrong shale type, or we boosted just a bit too much shale. In Natalia case, we tested with a softer shale to find possible Rogn sands in the graben structures and possible softer Cretaceous shale that lies on Jurassic sands. But that couldn't we find. But in the DigAVO, both Yttergryta and Natalia gave the right picture at well location with temperature 35 Celsius.

It's important to highlight is that chemical compaction by cementation occurs approximately at the depth where Yttergryta and Natalia reservoirs lie, just slightly above. Thereby, reservoirs that are slightly shallower will easily be unconsolidated and will more easily light up with hydrocarbon fillers. While reservoirs that are slightly deeper will be more cemented and stiffer, it can be difficult to "see" hydrocarbon fillings in them.

There are more cementation in Natalia than in Yttergryta, and that can be seen in the PeLe-results. This has affected the results for both of them, but most for Natalia that we can see on results from DigAVO. The interpretation of Natalia was challenging, because it was difficult to find so much hydrocarbons. In addition, it was difficult to see the structures at deeper depth.

In Natalia and Yttergryta there are mainly gas and gas condensate. But the condensate is almost like a light oil. Furthermore, the oil classification can be considered to be a certain probability for gas. It can for an example be a more dirty sand with gas may look like oil filled in seismic.

7 Conclusion

In this study we followed 3-stages of workflow, where we showed through three different software's that classification of fluids becomes more challenging when the rock becomes stiff. The element of cementation makes it more challenging to classify fluids at deeper depth. This was showcased in AVO classification of facies/fluids from Natalia and Yttergryta, while we took account to the burial history. There we highlighted the hydrocarbons of gas and condensate gas are in Yttergryta and Natalia.

References

Per Avseth and Ivan Lehocki. Combining burial history and rock-physics modeling to constrain AVO analysis during exploration. *NTNU, Tullow Oil, Lehocki Geospace*, pages 528–533, June 2016.

Knut Bjørnlykke and Jens Jahren. Sandstones and sandstone reservoirs. *Springer*, 2010.

Nordic CCS Competence Center, 2019. URL `https://data.geus.dk/nordiccs/geology.xhtml`.

Satinder Chopra and John Castagna. *AVO*. Tulsa, Oklahoma, U.S.A. : Society of Exploration Geophysicists, 2014, 2014.

Fritz Gassmann. *Ü*ber die elastizität porsöer medien. *Vierteljahrsschrift der Naturforschenden Gesellschaft in Zurich*, pages 1–23, Mars 1951.

Martin Landrø. *Seismic Data Acquisition and Imaging*, pages 1–100. NTNU, 2011.

NPD, 2019. URL `http://factpages.npd.no/FactPages/default.aspx?nav1=field&nav2=PageView%7CAll&nav3=4973114`.

Oljedirektoratet, 2019. URL `http://factpages.npd.no/ReportServer?/FactPages/PageView/discovery&rs:Command=Render&rc:Toolbar=false&rc:Parameters=f&NpdId=4972689&IpAddress=129.241.71.223&CultureCode=en`.

Andre Jancke Per Avseth and Frederik Horn. AVO Inversion in exploration - key learnings from a Norwegian Sea prospect. *Tullow Oil, NTNU, Qeye Labs*, May 2016.

Harald Flesche Per Avseth and Aart-Jan Wijngaarden. AVO classification of lithology and pore fluids constrained by rock physics depth trends. *Norsk Hydro Research Centre*, 2003.

Tapan Mukerji Per Avseth and Gary Mavko. Quantitative seismic interpretation – Applying rock-physics tools to seismic interpretation risk. *Cambridge University press*, 2005.

Steven Rutherford and Robert Williams. Amplitude-versus-offset variations in gas sands. *Society of Exploration Geophysicist*, pages 680–688, 1989.

R T Sheuy. A simplification of the Zoeppritz equations. *Geophysics Vol 50*, pages 609–614, 1985.

Olav Walderhaug. Kinetic modeling of quartz cementation and porosity loss in deeply buried sandstone reservoirs. *AAPG Bulletin*, pages 731–745, 1996.

Olav Walderhaug and Robert H Lander. Predicting porosity through simulating sandstone compaction and quartz cementation. *AAPG Bulletin*, page 433–449, Mars 1999.